Master's Thesis

Lund University
Faculty of Engineering
Division of Mathematical Physics

Non-local Transport Properties of a Sextuple Quantum Dot System in the Co-tunneling Regime

Author
Fredrik Norrman Brange

Supervisor
Peter Samuelsson

Co-supervisor
Ognjen Malkoc

June 3, 2014

Abstract

Quantum entanglement between electrons in nanostructures is a key concept of quantum information still waiting to be experimentally demonstrated. In this master's thesis we present and analyze the full counting statistics of the charge transfer of a sextuple quantum dot system which works as both entangler and detector of spatially separated electrons. Under certain resonance conditions the system operates in the co-tunneling regime, limiting environment-induced decoherence. By means of a generalized Schrieffer-Wolff transformation the co-tunneling dynamics are obtained from an effective Hamiltonian. Based on these results, a master equation is derived for the reduced density operator of the open sextuple dot system and used to compute the full counting statistics. We find that the system displays quantum coherent non-local transport properties and violates Bell's inequality. Consequently, the sextuple dot system could potentially be used to experimentally demonstrate entanglement between electrons as intended.

Acknowledgements

I would like to express my deep gratitude to my supervisor Peter Samuelsson, who has both given me the possibility to work with this interesting project and supported me when I have encountered difficulties. His intuition and knowledge have been very helpful during my work. I would also like to thank my co-supervisor Ognjen Malkoc for fruitful discussions, especially concerning the different approximations used for obtaining the full counting statistics.

Contents

Chapter 1

Introduction

The development of quantum mechanics during the last century was one of the most startling paradigm shifts in the history of physics. Describing phenomena where classical physics failed, quantum mechanics improved humanity's understanding of the fundamental laws of our world and laid the foundation for almost all modern physics.

Even though the predictions of quantum mechanics are incredibly consistent with experimental results, they sometimes contradict our own intuition of how we think the world works. *Quantum entanglement* is one of the most intriguing phenomena that appears in quantum mechanics and lacks any equivalent in classical physics. Entanglement is a concept where the properties of two or more particles are related to each other, such that knowledge of one entangled particle's property also reveals information about the other(s). This property can, for instance, be the spin, polarization or position of the particles. At first glance, this phenomenon may seem plain, but it turns out that entanglement has far-reaching consequences for one of the fundamental principles of classical physics, viz. *local realism*.

Based on the underlying contradiction between quantum mechanics and local realism, Einstein, Podolsky and Rosen questioned the actual effects of entanglement through the EPR paradox presented in 1935 [1]. Ever since, entanglement and its consequences have been subject of countless studies. In 1964, Bell showed [2] that in any local realistic theory quantum correlations between separated physical systems are bounded by an inequality, which can be violated if the predictions of quantum mechanics are valid. This inequality can be used to experimentally test if local realism or quantum mechanics is the superior theory consistent with our physical reality. Since the 1970s, a number of such experiments have been conducted, including the ones by Aspect et al. [3] and Zeilinger et al. [4–6]. The results supported quantum mechanics and the actual existence of quantum non-locality due to quantum entanglement.

Nevertheless, entanglement between *electrons* in nanostructures has not yet been demon-

strated. There are plenty of challenges associated with such experiments compared to those involving photons. Two typical kinds of entanglement between electrons are spin-entangled electrons and spatially entangled electrons. While spin is difficult to measure along an arbitrary direction, spatially entangled electrons are much more sensitive to decoherence due to a stronger coupling to the environment [7].

A general knowledge and understanding of entanglement between electrons is nonetheless important for the field of quantum information. In this thesis a new structure is presented and analyzed with the aim to make it possible to demonstrate entanglement between electrons experimentally. The structure is based on entanglement between spatially separated electrons and is operating in the co-tunneling regime. This regime makes it possible to minimize the time from production to detection of the entanglement. Consequently, environment-induced decoherence is limited.

In Ch. 2, quantum entanglement is explained in more detail as well as the principle of local realism and how these two concepts are related through Bell's inequality. The sextuple dot system is presented in Ch. 3 and its Hamiltonian is defined mathematically. In Ch. 4, a generalized Schrieffer-Wolff transformation is used to extract the interesting co-tunneling dynamics of the system. These results are used in Ch. 5 to derive a master equation in Lindblad form that describes the time evolution of the reduced density operator of the open sextuple dot system. From the master equation, all currents and fluctuations are determined using the concept of full counting statistics in Ch. 6. Finally, we show that the system displays quantum coherent non-local transport properties and violates Bell's inequality in Ch. 7. A final discussion and conclusion is provided in Ch. 8.

Chapter 2

Quantum Entanglement and Local Realism

In this chapter, a brief introduction is given in Sec. 2.1 to quantum entanglement, which is one of the key concepts in this thesis. In Sec. 2.2, the quantum mechanical violation of local realism is discussed. Experiments between entangled photons and electrons are described in Sec. 2.3 and 2.4, respectively.

2.1 Entanglement of a Singlet Spin State

The concept of quantum entanglement and its inconsistency with local realism is most clearly illustrated by considering a singlet spin state of two electrons. This example was originally formulated by Bohm and Aharonov in 1957 [8], and later used by Bell in his original formulation of Bell's inequality in 1964 [2].

A singlet state consists of two electrons, in the following denoted by A and B, that have a total spin equal to zero, which means that one of the electrons has spin up and the other has spin down. However, it is unknown which electron has which spin orientation. Therefore the total state is a superposition of the two possible combinations: particle A has spin up and particle B spin down, or particle A has spin down and particle B spin up. In Dirac notation, this state can be written as

$$|\Psi\rangle = \frac{1}{\sqrt{2}} \left(|\uparrow\rangle_A |\downarrow\rangle_B - |\downarrow\rangle_A |\uparrow\rangle_B \right) \tag{2.1}$$

where $|\uparrow\rangle_A$ denotes that particle A has spin up and so on. The minus sign is a consequence of the anti-symmetry of fermionic wavefunctions. The prefactor $\frac{1}{\sqrt{2}}$ is a normalization constant.

Let's now imagine that the two singlet electrons are spatially separated by an arbitrary large distance. By using some measurement devices, such as Stern-Gerlach magnets, the spin of each electron can be measured separately along some arbitrary direction. Due to the properties of the singlet state, the outcome of the measurements will be anti-correlated if the basis is the same for the two measurements.

This means that we know the spin orientation of particle B already at the moment we measure the spin of particle A, and vice versa. At first glance, this might not seem to be an intriguing phenomenon, because the spin orientation of each particle may have been assigned already at the moment the particles were separated.

However, the remarkable result appears due to the possibility of having different bases for the measurements of the spin orientations. The correlation between the outcome of the measurements on each electron's spin will then depend on the choice of bases. This choice of bases can be made long after the two particles were separated. It is therefore reasonable to assume that the particles do not know what the outcome of the measurements will be at the moment they are separated.

Nonetheless, particle B will immediately "know" the outcome of the first measurement on particle A, even though the two particles are separated by an arbitrary large distance. It is this peculiar result of entanglement that is inconsistent with local realism, which is discussed in the next section.

More generally, entanglement can involve other properties than spin, such as polarization or position. The former is typically used in experiments involving entangled photons. Mathematically speaking, an entangled state is the opposite of a separable state. This means that an entangled state cannot be written as a product of pure states, i.e., the local state of each particle. The singlet state in Eq. (2.1) is just one example of this.

2.2 Local Realism, EPR Paradox and Bell's Inequality

The peculiar results of entanglement were questioned by Einstein, Podolsky and Rosen in 1935 through the so-called EPR paradox [1]. They claimed that quantum mechanics was an incomplete theory since it violates local realism, which they considered to be a superior principle of our physical reality.

Local realism combines two different concepts. First, it includes *locality*, which means that measurements on space-like separated events cannot affect each other. For instance, the outcomes of the two Stern-Gerlach magnets cannot affect each other until at least the time it takes for light to travel between them has elapsed. Second, it includes *reality*, which means that there exists an external reality with definite properties. These properties are not dependent on whether we observe them or not.

As pointed out in the EPR paradox, the concept of entanglement has far-reaching consequences that are inconsistent with local realism [9]. Consequently, in the EPR paradox it was argued that quantum mechanics was an incomplete theory missing some hidden variables. These hidden variables would, according to EPR, complete quantum mechanics and make it finally consistent with local realism.

For a long time, it was not clear if it was possible at all to experimentally test if local realism really prevails over quantum mechanics as EPR claimed. Several attempts were made to theoretically prove that any hidden variable theory would be inconsistent with quantum mechanics. The most famous one was probably von Neumann's impossibility proof in 1932 [10], three years before the EPR paradox was presented. However, Bell proved in 1966 [11] that von Neumann's assumptions were not valid for non-commuting operators, which are exactly the ones of interest. Already in 1952, Bohm had presented [12, 13] a local hidden variable theory that contradicted von Neumann's proof.

In 1964, Bell finally showed [2] that in any local realistic theory quantum correlations between separated physical systems are bounded by an inequality. Quantum mechanics, on the other hand, predicts that this inequality can be violated. This insight made it possible to experimentally test if local realism prevails over quantum mechanics. This paved the way for a whole new series of experiments from the 1970s up until today.

While Bell's inequality concerned the singlet state specifically, a more generalized inequality was presented by Clauser, Horne, Shimony and Holt in 1969 [14]. In the so-called CHSH inequality, named after the four authors, one considers two measurements on two different particles. The probabilities to get different combinations of outcomes in the two measurements are denoted by P_{++}, P_{+-}, P_{-+} and P_{--}, where for instance P_{++} is the probability to get spin up in both measurements in the example with the singlet state. The so-called quantum correlation, denoted by E, is defined by

$$E = \frac{P_{++} + P_{--} - P_{+-} - P_{-+}}{P_{++} + P_{--} + P_{+-} + P_{-+}} \tag{2.2}$$

The probabilities will of course depend on the choice of bases. Hence, for each experimental setup where θ_1 is the angle of the basis of the first measurement and θ_2 is the angle of the basis of the second measurement, a certain expectation value $E_{\theta_1\theta_2}$ is obtained. The CHSH inequality is constructed by conducting four experiments with different setups, where two different bases θ_1 and θ_1' are used for the first measurement and another two θ_2 and θ_2' are used for the second measurement. Every experiment combines one of the two former bases with one of the two latter. The Bell parameter is then defined by

$$S = |E_{\theta_1\theta_2} - E_{\theta_1\theta_2'} + E_{\theta_1'\theta_2} + E_{\theta_1'\theta_2'}| \tag{2.3}$$

Based on local realism, this quantity can never exceed a maximum value of 2. However, quantum mechanics predicts that this quantity can reach values as high as $2\sqrt{2}$. This generalized formulation of Bell's inequality will be used in Ch. 7 to show that the sextuple dot system violates local realism, which demonstrates the actual existence of entanglement.

2.3 Experiments Involving Photons

As already mentioned, Bell's inequality opened up a whole new field of research in experimental physics. Since the 1970s, a number of experiments have been conducted with entangled photons to show that local realism can be violated. However, the experiments required a clever design to show non-local effects and to avoid different kinds of loophole-inducing assumptions.

The first experiment was performed by Freedman and Clauser in 1972 [15] and the results were in favor of quantum mechanics. In 1973, Holt and Pipkin conducted an experiment that was in favor of local realism, but Clauser found in 1976 that this was an effect of stresses in the optics [9].

Later experiments aimed to eliminate different kinds of loophole-inducing assumptions. For instance, the measurements had to be performed outside each other's future light cones to exclude the locality principle as a necessary assumption. Experiments by Aspect et al. in the 1980s tried to close this so-called locality loophole [3]. However, it turned out that the distance between the polarizers used in the experiment was too small to guarantee a truly random orientation reseting. Weihs et al. became the first group to finally close the locality loophole in 1998 [4].

Other loopholes have been addressed in later experiments. The freedom-of-choice loophole was addressed in 2010 by Scheidl et al. and favored quantum mechanics [5]. A third loophole, the fair-sampling assumption, was closed together with the locality loophole in 2013 by Giustina et al. [6]. However, all loopholes have not yet been closed in one and the same experiment [5].

2.4 Experiments Involving Electrons

Experiments involving entangled electrons instead of photons to show the effects of entanglement have yet to become reality. The main reason is that electrons interact with the environment much more than photons [7]. The coupling to the environment gives rise to decoherence that impairs the entanglement. This limits the chances of separating electrons over large distances and long times, and still keep the entanglement intact.

Instead of using polarization as entanglement property, spin or position is used for electrons. Spin-entangled electrons are less exposed to decoherence than spatially entangled electrons due to a weaker coupling to the environment. On the other hand, it is difficult to measure spin along an arbitrary direction, whereas it is relatively easy to detect spatially separated electrons.

If the time between production and detection of the entanglement is short, environment-induced decoherence can be limited. This could potentially allow for the use of spatially separated electrons and still keep the entanglement intact. The system presented in the next chapter is based on this idea.

Chapter 3

The Sextuple Dot System

In this chapter, the sextuple dot system is first described in detail in Sec. 3.1. In Sec. 3.2, the second quantization formalism is introduced as a powerful tool to describe many-particle systems in quantum theory. This formalism is used in Sec. 3.3 to formulate the Hamiltonian of the sextuple dot system, which is the main result of this chapter.

3.1 Description of the System

As pointed out in the introduction, the purpose of the sextuple dot system is to make it possible to experimentally demonstrate quantum entanglement between electrons in a nanostructure. To do this we use a system consisting of six quantum dots, each coupled to a lead as shown in Fig. 3.1. The center leads 1–2 are kept at a bias V, while the side leads 3–6 are grounded. All leads are kept at the same temperature $k_BT \ll eV$. Only one energy level is assumed to be within the bias window in each dot and a strong on-site Coulomb repulsion prohibits two electrons from occupying the same spin-degenerated level. Consequently, only one single electron can occupy each dot.

The electrons enter the system by tunneling to the center dots QD1 and QD2, respectively, from the center leads. The high bias regime guarantees that the electron transport only occurs in one direction; from the center leads via the sextuple dot system out to the side leads on each side.

The dot-level energies are tuned such that sequential tunneling, i.e., when single electrons tunnel at a time, from the center dots (QD1–2) to any of the side dots (QD3–6) is off-resonance and thus weak. However, the energy levels of the center dots are matched to the side dots such that *co-tunneling*, i.e., when the two electrons in the center dots tunnel simultaneously, is at resonance and dominates the transport. The resonance condition is

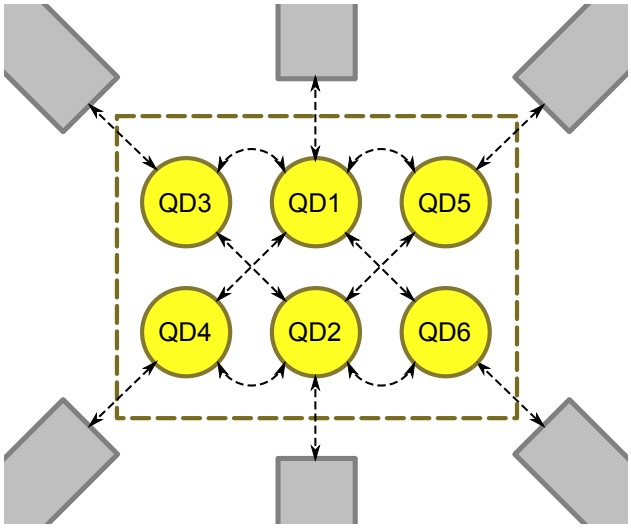

Figure 3.1: The sextuple dot system with the leads. The dashed box marks the open system.

further discussed in Sec. 7.1.

A strong Coulomb repulsion between the dots on each side prohibits the two electrons from tunneling to the same side. In other words, one of the two electrons will always tunnel to the left and one to the right. The electrons are detected at each side dot, which consequently act like detectors. There are several different ways of detecting the electrons, such as using quantum point contacts to detect single electrons or detecting the currents through the leads. The quantum correlations between the side dots are studied. If the entanglement had included sequential tunneling, the time from production to detection of the entanglement would have been rather long and exposed to decoherence due to the coupling to the environment. This would have resulted in a loss of the entanglement. However, since the sextuple dot system operates in the co-tunneling regime, the time from production to detection is short and there is in principle no time for the surroundings to affect the entanglement.

For simplicity, tunneling is assumed to be allowed only between the center dots and the side dots. The coupling between a dot and its lead is much stronger than the coupling between two dots. The different coupling strengths give rise to three different time scales that can be distinguished. The longest one is the co-tunneling, i.e., the time from the moment two center dots have been occupied until they are empty again. The shortest one is the time scale during which the tunneling between a dot and its lead takes place. In between is the time scale during which the center dots are empty.

The assumptions leading to the different time scales are very important since they will be

used to simplify the problem. For instance, they imply that there can only be two electrons at most at the same time in the sextuple dot system. As will be shown later, the assumptions also make it possible to neglect so-called elastic co-tunneling.

Entanglement

As already pointed out, one of the two electrons in the center dots will always tunnel to the left and one to the right. However, we do not know which of the two electrons tunnels to which side. This gives rise to entanglement effects similar to the ones discussed in the example of the singlet state in Sec. 2.1. Until a measurement is performed, the system will be in a superposition of two different pure states. For example, if the two electrons in the center dots tunnel to QD3 and QD6, respectively, the total state will be given by

$$|\Psi\rangle = \frac{1}{\sqrt{2}} \left(|3\rangle_1 |6\rangle_2 - |6\rangle_1 |3\rangle_2 \right) \tag{3.1}$$

where $|3\rangle_1$ denotes that the particle in QD1 has tunneled to QD3 and so on. This state is completely analogous to the singlet state in Eq. (2.1). Since the state cannot be rewritten into a separable product of pure states, it is entangled.

By tuning the tunneling amplitudes between the center dots and the side dots, the probability that a particle tunnels to a certain side dot can be changed. This corresponds to changing the basis of the spin measurement in the example of the singlet state.

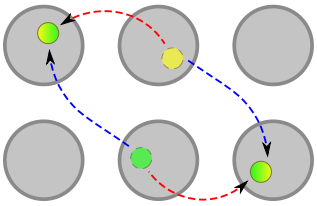

Figure 3.2: Entanglement arises when two electrons in the center dots co-tunnel to two of the side dots. It is not known if the yellow particle tunnels to the left and the green particle to the right (red arrows) or if the yellow particle tunnels to the right and the green particle to the left (blue arrows). Therefore the system will be in a superposition between the two cases resulting in an entangled state.

3.2 Second Quantization Formalism

Second quantization formalism is a powerful tool for handling many-particle systems mathematically. In the following a short and concise summary of this formalism is provided. A more comprehensive introduction can be found in, e.g., Bruus and Flensberg [16].

The basis for the second quantization formalism is the creation operators $a_i^\dagger$ and the annihilation operators a_i, which create and annihilate, respectively, a particle in a state with quantum number i, where i may be a set of numbers.

The *commutator* of two operators A and B is defined by $[A,B]_- = AB - BA$, whereas the *anti-commutator* is defined by $[A,B]_+ = AB + BA$. If the (anti-)commutator fulfills the condition $[A,B]_{-(+)} = 0$, the two operators are said to be (anti-)commuting. It follows directly from the definitions that $[A,B]_{+(-)} = (-)[B,A]_{+(-)}$. The following commutator rules can be easily derived:

$$[AB,C]_- = A[B,C]_+ - [C,A]_+B \qquad [AB,C]_- = A[B,C]_- - [C,A]_-B \tag{3.2}$$

The creation and annihilation operators for fermions fulfill the following canonical anti-commutation relations as a consequence of their anti-symmetric wavefunctions:

$$[a_i, a_j^\dagger]_+ = \delta_{ij} \qquad [a_i^\dagger, a_j^\dagger]_+ = [a_i, a_j]_+ = 0 \tag{3.3}$$

where the Kronecker delta function δ_{ij} has been introduced. Note that creation as well as annihilation operators acting on different states are anti-commuting.

In this thesis, $\{d_\alpha^\dagger, d_\alpha\}$ will denote operators acting on the state of *dot* α and $\{c_{k\alpha}^\dagger, c_{k\alpha}\}$ will denote operators acting on the state of *lead* α with wavenumber k. For the number operator $n_\alpha \equiv d_\alpha^\dagger d_\alpha$, the following commutator relations hold [17, 18]:

$$[d_\alpha, n_\alpha]_- = d_\alpha \qquad [d_\alpha^\dagger, n_\alpha]_- = -d_\alpha^\dagger \qquad [n_\alpha, n_{\alpha'}]_- = 0 \qquad n_\alpha^2 = n_\alpha \tag{3.4}$$

3.3 Formulation of the Hamiltonian

Returning to the sextuple dot system, the Hamiltonian of the system can now be formulated using the second quantization formalism. The Hamiltonian H will be split into two parts, (1) H_0 describing the unperturbed system consisting of the quantum dots, the leads and their mutual coupling, and (2) V^{dd} describing the sequential tunneling between the quantum dots. Since the latter interaction is weak compared to the former, V^{dd} will be considered as a perturbation in Ch. 4, where the co-tunneling dynamics are extracted by means of a generalized Schrieffer-Wolff transformation.

Hamiltonian of the Unperturbed System

The unperturbed Hamiltonian consists of four parts. The first part describes the single-particle energy levels ϵ_α of the quantum dots. As already mentioned, only one level is assumed to be within the energy window, leaving the possibility of having two electrons at most in a dot due to spin degeneracy and the Pauli principle. However, the on-site Coulomb repulsion between two electrons in the same dot is assumed to be much larger than any other relevant energy scale of the system. Hence, each dot can only contain one electron at most. The effect of the spin is taken into account by a renormalization that will only affect the rate at which the electrons enter the system. The Hamiltonian H^d for the sum of the six isolated dots becomes then

$$H^d = \sum_\alpha \epsilon_\alpha d_\alpha^\dagger d_\alpha = \sum_\alpha \epsilon_\alpha n_\alpha \tag{3.5}$$

The second part consists of an analog expression for each lead. The only qualitative difference is that the density of states differs from the dots. An additional quantum number, the wavenumber k, describes all states in each lead. The Hamiltonian becomes then

$$H^c = \sum_{k\alpha} \epsilon_{k\alpha} c_{k\alpha}^\dagger c_{k\alpha} \tag{3.6}$$

where the energy levels of the leads are denoted by $\epsilon_{k\alpha}$. Since the distance between the quantum dots is small, the interaction strength $U_{\alpha\alpha'}$ of the Coulomb repulsion between electrons in two different dots α and α' has to be included as well. This is taken into account by the third part, the so-called capacitive Hamiltonian:

$$H^{\text{cap}} = \sum_{\alpha\alpha'} \frac{1}{2} U_{\alpha\alpha'} d_\alpha^\dagger d_{\alpha'}^\dagger d_{\alpha'} d_\alpha = \sum_{\alpha\alpha'} \frac{1}{2} U_{\alpha\alpha'} n_\alpha n_{\alpha'} \tag{3.7}$$

where $U_{\alpha\alpha'} = U_{\alpha'\alpha}$ and $U_{\alpha\alpha} = 0$. To avoid double counting, a prefactor of $\frac{1}{2}$ has been added. The fourth and last part corresponds to the tunneling between the leads and the dots:

$$V^{dc} = \sum_{k\alpha} \left(t_{k\alpha} c_{k\alpha}^\dagger d_\alpha + t_{k\alpha}^* d_\alpha^\dagger c_{k\alpha} \right) \tag{3.8}$$

where $t_{k\alpha}$ is the tunneling amplitude between dot α and its lead. The total unperturbed Hamiltonian is then given by the sum of the four different parts:

$$H_0 = \sum_{\alpha} \epsilon_\alpha n_\alpha + \sum_{k\alpha} \epsilon_{k\alpha} c^\dagger_{k\alpha} c_{k\alpha} + \sum_{\alpha\alpha'} U_{\alpha\alpha'} n_\alpha n_{\alpha'} + \sum_{k\alpha} \left(t_{k\alpha} c^\dagger_{k\alpha} d_\alpha + t^*_{k\alpha} d^\dagger_\alpha c_{k\alpha} \right) \tag{3.9}$$

Hamiltonian of the Perturbation

The perturbation V^{dd} describes the tunneling between the six dots. This allows electrons to move from one dot to another. If $t_{\alpha\alpha'}$ denotes the tunneling amplitude between dot α and dot α', the Hamiltonian is given by

$$V^{dd} = \sum_{\alpha\alpha'} \frac{1}{2} \left(t_{\alpha\alpha'} d^\dagger_\alpha d_{\alpha'} + t^*_{\alpha\alpha'} d^\dagger_{\alpha'} d_\alpha \right) \tag{3.10}$$

Note that $t^*_{\alpha'\alpha} = t_{\alpha\alpha'}$ and $t_{\alpha\alpha} = 0$, since tunneling between a dot and itself is not possible. Only t_{13}, t_{14}, t_{15}, t_{16}, t_{23}, t_{24}, t_{25}, t_{26} and their complex conjugates are non-zero, because only tunneling between any of the two center dots and any of the four side dots is allowed.

Chapter 4

Schrieffer-Wolff Transformation

In cases where sequential tunneling of single electrons is suppressed (off-resonance), higher-order processes such as co-tunneling become crucial for the dynamic behavior of the quantum system. These dynamics can be extracted from the Hamiltonian by means of a generalized Schrieffer-Wolff transformation. The transformation projects the Hamiltonian H onto the low-energy sector yielding an effective Hamiltonian H_{eff}. The aim of this chapter is to use this concept to eliminate the sequential tunneling V^{dd} between the dots in the total Hamiltonian $H = H_0 + V^{dd}$ from Sec. 3.3. For simplicity, this perturbation will be denoted by V in the rest of the chapter.

The Schrieffer-Wolff transformation was originally used to show how the Hamiltonian of the Anderson model is related to the Kondo Hamiltonian [19]. It has later been applied to different kinds of systems, including structurally similar ones such as double quantum dots [17, 20–22]. More generally, the Schrieffer-Wolff transformation U is a unitary transformation that transforms a Hamiltonian H into an effective Hamiltonian H_{eff} given by

$$H_{\text{eff}} = UHU^\dagger = \mathrm{e}^S H \mathrm{e}^{-S} \tag{4.1}$$

where the anti-Hermitian generator S of the transformation has been introduced. The effective Hamiltonian takes into account higher-order processes that become important when the sequential tunneling is suppressed. A more rigorous mathematical analysis of the transformation can be found in [23]. Using Baker-Campbell-Hausdorff formula [19], Eq. (4.1) can be expressed as

$$H_{\text{eff}} = \mathrm{e}^S H \mathrm{e}^{-S} = H + [S,H]_- + \frac{1}{2}[S,[S,H]_-]_- + \ldots \frac{1}{n!}[S,[S,\ldots[S,H]_-\ldots]_-]_- + \ldots \tag{4.2}$$

To eliminate V to first order in this expansion, the following condition has to be fulfilled

$$V + [S, H_0]_- = 0 \tag{4.3}$$

One of the practical difficulties with the Schrieffer-Wolff transformation is to find an explicit expression for the generator S from Eq. (4.3).

4.1 Generator S of the Transformation

In this section, an explicit expression for the generator S is presented. A derivation of this generator is provided in Appendix A.

The generator is first determined when the dot-lead coupling is neglected. The generator is then given by (cf. Eq. (3.10))

$$S = \sum_{\alpha\alpha'} \frac{1}{2} E_{\alpha\alpha'} \left(t_{\alpha\alpha'} d_\alpha^\dagger d_{\alpha'} - t_{\alpha\alpha'}^* d_{\alpha'}^\dagger d_\alpha \right) \tag{4.4}$$

with

$$E_{\alpha\alpha'} = \sum_{B \in \mathbb{B}} \left(\frac{1}{\epsilon_B} \prod_{\beta \in B} n_\beta \prod_{\beta \notin B} (1 - n_\beta) \right) \tag{4.5}$$

where $\mathbb{B}$ is the set of all possible combinations of occupied dot states, except the dot states α and α', and ϵ_B is the energy difference between the final state and the initial state when tunneling takes place between dot α and dot α' with the occupation combination B. A proof is provided in Appendix A. Note that $E_{\alpha\alpha'} = -E_{\alpha'\alpha}$ and $E_{\alpha\alpha'}^\dagger = E_{\alpha\alpha'}$. As seen in Eq. (4.4), the generator is very similar to the perturbation V, but with the additional $E_{\alpha\alpha'}$ operators.

When the dot-lead coupling is taken into account, additional terms will appear in the denominator, adjusting the values of ϵ_B. However, since the sequential tunneling is off-resonance, the denominator ϵ_B is far from zero. A small additional value to the denominator proportional to the weak coupling strength between the dots and the leads will not have any substantial effect. Hence, the effect of the dot-lead coupling is negligible and the previous expression of the generator still holds.

4.2 Effective Hamiltonian of First Order

If higher-order terms are neglected in Eq. (4.2), the effective Hamiltonian is given by

$$H_{\text{eff}} \approx H_0 + \frac{1}{2}[S, V]_- \tag{4.6}$$

In other words, the additional term to the unperturbed Hamiltonian is in the form $[S, V]_-$. The effective Hamiltonian can therefore be obtained by computing a number of commutators.

In the remaining part of this section, α_1 and α_2 denote arbitrary center dots, whereas β_1 and β_2 denote arbitrary side dots. The new dynamics contained in the commutator $\frac{1}{2}[S, V]_-$ can then be divided into three kinds of commutators for a given term $\frac{1}{2}\left(t_{\alpha_1\beta_1} d^\dagger_{\alpha_1} d_{\beta_1} + t^*_{\alpha_1\beta_1} d^\dagger_{\beta_1} d_{\alpha_1}\right)$ in V.

Renormalization Terms

The first kind of term is given by

$$\begin{aligned}\frac{1}{8}[E_{\alpha_1\beta_1}(t_{\alpha_1\beta_1} d^\dagger_{\alpha_1} d_{\beta_1} - t^*_{\alpha_1\beta_1} d^\dagger_{\beta_1} d_{\alpha_1}), t_{\alpha_1\beta_1} d^\dagger_{\alpha_1} d_{\beta_1} + t^*_{\alpha_1\beta_1} d^\dagger_{\beta_1} d_{\alpha_1}]_- = \\ = \frac{1}{4}|t_{\alpha_1\beta_1}|^2 E_{\alpha_1\beta_1}(n_{\alpha_1} - n_{\beta_1})\end{aligned} \tag{4.7}$$

where $E_{\alpha_1\beta_1}$ is given by Eq. (4.5). Apparently, this kind of term only consists of number operators. It can thus be eliminated by means of a renormalization of the single-particle energy levels ϵ_α and the interaction strengths $U_{\alpha\alpha'}$. This does not affect the dynamic behavior of the sextuple dot system qualitatively. In the following chapters all affected parameters are assumed to be renormalized to take this effect into account.

Elastic Co-tunneling Terms

The second kind of term is

$$\begin{aligned}\frac{1}{8}[E_{\alpha_1\beta_2}(t_{\alpha_1\beta_2} d^\dagger_{\alpha_1} d_{\beta_2} - t^*_{\alpha_1\beta_2} d^\dagger_{\beta_2} d_{\alpha_1}), t_{\alpha_1\beta_1} d^\dagger_{\alpha_1} d_{\beta_1} + t^*_{\alpha_1\beta_1} d^\dagger_{\beta_1} d_{\alpha_1}]_- = \\ = -\frac{1}{8} E_{\alpha_1\beta_2}(n_{\beta_1} \to n_{\alpha_1})(t_{\alpha_1\beta_2} t^*_{\alpha_1\beta_1} d^\dagger_{\beta_1} d_{\beta_2} + t^*_{\alpha_1\beta_2} t_{\alpha_1\beta_1} d^\dagger_{\beta_2} d_{\beta_1})\end{aligned} \tag{4.8}$$

and

$$\begin{aligned}\frac{1}{8}[E_{\alpha_2\beta_1}(t_{\alpha_2\beta_1} d^\dagger_{\alpha_2} d_{\beta_1} - t^*_{\alpha_2\beta_1} d^\dagger_{\beta_1} d_{\alpha_2}), t_{\alpha_1\beta_1} d^\dagger_{\alpha_1} d_{\beta_1} + t^*_{\alpha_1\beta_1} d^\dagger_{\beta_1} d_{\alpha_1}]_- = \\ = -\frac{1}{8} E_{\alpha_2\beta_1}(n_{\alpha_1} \to n_{\beta_1})(t_{\alpha_2\beta_1} t^*_{\alpha_1\beta_1} d^\dagger_{\alpha_2} d_{\alpha_1} + t^*_{\alpha_2\beta_1} t_{\alpha_1\beta_1} d^\dagger_{\alpha_1} d_{\alpha_2})\end{aligned} \tag{4.9}$$

where $E_{\alpha_1\beta_2}(n_{\beta_1} \to n_{\alpha_1})$ denotes the operator $E_{\alpha_1\beta_2}$ given by Eq. (4.5), but with n_{β_1} replaced by n_{α_1}.

Both of these terms contribute with new dynamics to the effective Hamiltonian, namely the possibility of having elastic co-tunneling. In Fig. 4.1, an example of elastic co-tunneling is shown. However, the elastic co-tunneling is negligible. For instance, if an electron tunnels to a side dot, it will instantaneously continue to tunnel to the lead, since the dot-lead coupling is stronger than the couplings between the dots. The same argument applies to the situation when only one of the center dots is occupied. In this case, the other center dot will more or less instantaneously be filled by an electron before any elastic co-tunneling can take place. When both center dots are filled, they will favor inelastic co-tunneling instead of elastic co-tunneling because the former is at resonance.

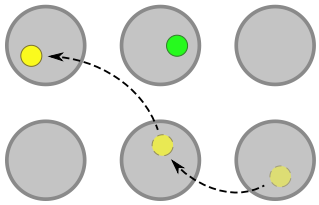

Figure 4.1: Elastic co-tunneling. The electron (yellow dot) co-tunnels with itself and moves in this case from QD6 to QD3 via QD2. This can happen in both presence and absence of another electron (green dot).

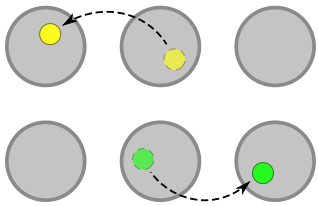

Figure 4.2: Inelastic co-tunneling. Two electrons tunnel together. Two electrons in the center dots tunneling to one side dot on each side is the only important co-tunneling mechanism for the dynamics of the sextuple dot system.

Inelastic Co-tunneling Terms

The third kind of term is given by

$$\begin{aligned}
&\frac{1}{8}[E_{\alpha_2\beta_2}(t_{\alpha_2\beta_2}d^\dagger_{\alpha_2}d_{\beta_2} - t^*_{\alpha_2\beta_2}d^\dagger_{\beta_2}d_{\alpha_2}), t_{\alpha_1\beta_1}d^\dagger_{\alpha_1}d_{\beta_1} + t^*_{\alpha_1\beta_1}d^\dagger_{\beta_1}d_{\alpha_1}]_- = \\
&= \frac{1}{8}\left(\frac{1}{\epsilon_{\alpha_2} + U_{\alpha_1\alpha_2} - \epsilon_{\beta_2} - U_{\alpha_1\beta_2}} - \frac{1}{\epsilon_{\alpha_2} + U_{\alpha_2\beta_1} - \epsilon_{\beta_2} - U_{\beta_1\beta_2}}\right)\Big(t_{\alpha_1\beta_1}t_{\alpha_2\beta_2}d^\dagger_{\alpha_2}d^\dagger_{\alpha_1}d_{\beta_1}d_{\beta_2} \\
&\qquad + t^*_{\alpha_1\beta_1}t^*_{\alpha_2\beta_2}d^\dagger_{\beta_2}d^\dagger_{\beta_1}d_{\alpha_1}d_{\alpha_2} + t^*_{\alpha_1\beta_1}t_{\alpha_2\beta_2}d^\dagger_{\alpha_2}d^\dagger_{\beta_1}d_{\alpha_1}d_{\beta_2} + t_{\alpha_1\beta_1}t^*_{\alpha_2\beta_2}d^\dagger_{\beta_2}d^\dagger_{\alpha_1}d_{\beta_1}d_{\alpha_2}\Big) \quad (4.10)
\end{aligned}$$

This term yields co-tunneling with two particles, i.e., inelastic co-tunneling. An example of inelastic co-tunneling is shown in Fig. 4.2. The two last inelastic co-tunneling terms correspond to co-tunneling with an electron in a center dot and an electron in a side dot, which is a negligible process. The two first inelastic co-tunneling terms are thus those of interest. They correspond to co-tunneling between the center dots and the side dots.

The two-particle co-tunneling amplitude $t_{\alpha\alpha'\beta\beta'}$ can be introduced as

$$t_{\alpha\alpha'\beta\beta'} = \frac{1}{8}\left(\frac{1}{\epsilon_{\alpha'} + U_{\alpha\alpha'} - \epsilon_{\beta'} - U_{\alpha\beta'}} - \frac{1}{\epsilon_{\alpha'} + U_{\alpha'\beta} - \epsilon_{\beta'} - U_{\beta\beta'}}\right)t_{\alpha\beta}t_{\alpha'\beta'} \quad (4.11)$$

In the following, $x \in \{3, 4\}$ will denote a left side dot and $y \in \{5, 6\}$ will denote a right side dot. The total co-tunneling amplitude between the center dots QD1–2 and each pair of a left side dot x and a right side dot y is then given by the sum of four different co-tunneling amplitudes that are obtained by permuting the indices in Eq. (4.11):

$$\begin{aligned}
t_{12xy} = \frac{1}{8}\Bigg(&\Big(\frac{1}{\epsilon_2 + U_{12} - \epsilon_y - U_{1y}} - \frac{1}{\epsilon_2 + U_{2x} - \epsilon_y - U_{xy}} \\
&+ \frac{1}{\epsilon_1 + U_{12} - \epsilon_x - U_{2x}} - \frac{1}{\epsilon_1 + U_{1y} - \epsilon_x - U_{xy}}\Big)t_{1x}t_{2y} \\
&- \Big(\frac{1}{\epsilon_1 + U_{12} - \epsilon_y - U_{2y}} - \frac{1}{\epsilon_1 + U_{1x} - \epsilon_y - U_{xy}} \\
&+ \frac{1}{\epsilon_2 + U_{12} - \epsilon_x - U_{1x}} - \frac{1}{\epsilon_2 + U_{2y} - \epsilon_x - U_{xy}}\Big)t_{1y}t_{2x}\Bigg) \quad (4.12)
\end{aligned}$$

4.3 Approximative Effective Hamiltonian

When neglecting the elastic co-tunneling terms, the effective Hamiltonian can be written in the following form:

$$H_{\text{eff}} = \sum_{\alpha} \epsilon_{\alpha} d_{\alpha}^{\dagger} d_{\alpha} + \sum_{k\alpha} \epsilon_{k\alpha} c_{k\alpha}^{\dagger} c_{k\alpha} + \sum_{\alpha\alpha'} \frac{1}{2} U_{\alpha\alpha'} n_{\alpha} n_{\alpha'} + \sum_{k\alpha} \left(t_{k\alpha} c_{k\alpha}^{\dagger} d_{\alpha} + t_{k\alpha}^{*} d_{\alpha}^{\dagger} c_{k\alpha} \right) + \sum_{xy} \left(t_{12xy} d_1^{\dagger} d_2^{\dagger} d_x d_y + t_{12xy}^{*} d_y^{\dagger} d_x^{\dagger} d_2 d_1 \right) \quad (4.13)$$

where the two-particle co-tunneling amplitudes t_{12xy} are given by Eq. (4.12). Note that ϵ_{α} and $U_{\alpha\alpha'}$ now denote the renormalized quantities.

Chapter 5

Master Equation in Lindblad Form

In this chapter, a master equation in Lindblad form is derived for the open sextuple dot system. The master equation describes the time evolution of the reduced density operator $\rho(t)$ of the open system taking into account the interaction between the sextuple dots and their surroundings, also called the bath for historical reasons. The derived master equation is then formulated in matrix representation and used for computing the full counting statistics in Ch. 6.

5.1 Density Operator

The density operator ρ (which has nothing to do with mass density) can be seen as a generalization of a pure state $|\Psi\rangle$. In contrast to a pure state, the density operator can describe quantum systems that are in a mixed state. The density operator can be written as

$$\hat{\rho} = \sum_{kk'} \hat{\rho}_{k,k'} |k\rangle\langle k'| \tag{5.1}$$

where $\{|k\rangle\}$ is a set of pure states, which do not need to be orthogonal. More mathematically, the density operator is defined as a positive operator with trace equal to one [24]. The diagonal elements $\hat{\rho}_{k,k}$ of the density operator are called *populations* since they correspond to the probability that the system is found in a specific state. The off-diagonal elements $\hat{\rho}_{k,k'}$ are called *coherences* and play a central role for describing interference.

5.2 Derivation of the Master Equation

There are several different ways of deriving a master equation. The following one is based on Gardiner and Zoller [25] and follows the same approach as Samuelsson [26]. It uses the von Neumann equation as its starting point. By changing between the Schrödinger picture and the interaction picture, a master equation is finally obtained for the time evolution of the open sextuple dot system.

The time evolution of any closed system is described by the von Neumann equation. Since the system can be in a combination of pure states, it is described by a density operator $\hat{\rho}(t)$ as introduced in the previous section. The open sextuple dot system S (not to be confused with the generator S in Ch. 4) and its bath B, consisting of the leads, together constitute a closed system, meaning that the time evolution of the density operator $\hat{\rho}(t)$ of the entire system is given by the von Neumann equation, i.e.,

$$\frac{d\hat{\rho}(t)}{dt} = -\frac{i}{\hbar}[H, \hat{\rho}(t)]_- \tag{5.2}$$

where $H = H_S + H_B + H_T$ with

$$H_S = \sum_\alpha \epsilon_\alpha d_\alpha^\dagger d_\alpha + \sum_{\alpha\alpha'} \frac{1}{2} U_{\alpha\alpha'} n_\alpha n_{\alpha'} + \sum_{xy} \left(t_{12xy} d_1^\dagger d_2^\dagger d_x d_y + t_{12xy}^* d_y^\dagger d_x^\dagger d_2 d_1 \right)$$

$$H_B = \sum_{k\alpha} \epsilon_{k\alpha} c_{k\alpha}^\dagger c_{k\alpha}$$

$$H_T = \sum_{k\alpha} \left(t_{k\alpha} c_{k\alpha}^\dagger d_\alpha + t_{k\alpha}^* d_\alpha^\dagger c_{k\alpha} \right)$$

In the interaction picture the density operator $\hat{\rho}_I(t)$ for the entire system is per definition [27] related to $\hat{\rho}(t)$ in the Schrödinger picture by

$$\hat{\rho}_I(t) = e^{i(H_S+H_B)t/\hbar} \hat{\rho}(t) e^{-i(H_S+H_B)t/\hbar} \tag{5.3}$$

and its time evolution is subsequently described by the von Neumann equation in the interaction picture

$$\frac{d\hat{\rho}_I(t)}{dt} = -\frac{i}{\hbar}[H_T(t), \hat{\rho}_I(t)]_- \tag{5.4}$$

with the tunneling Hamiltonian in the interaction picture defined by

$$H_T(t) = e^{i(H_S+H_B)t/\hbar} H_T e^{-i(H_S+H_B)t/\hbar} \tag{5.5}$$

By integrating Eq. (5.4), the following relation is obtained:

$$\hat{\rho}_I(t) - \hat{\rho}_I(0) = -\frac{i}{\hbar}\int_0^t dt'[H_T(t'), \hat{\rho}_I(t')]_- \tag{5.6}$$

Using the first Born approximation [28], this expression is inserted back into Eq. (5.4) yielding

$$\frac{d\hat{\rho}_I(t)}{dt} = -\frac{i}{\hbar}[H_T(t), \hat{\rho}_I(0)]_- - \frac{1}{\hbar^2}\int_0^t dt'[H_T(t), [H_T(t'), \hat{\rho}_I(t')]_-]_- \tag{5.7}$$

However, it is not $\hat{\rho}(t)$ (or $\hat{\rho}_I(t)$) itself that is of interest, but the reduced density operator $\rho(t)$ of the open sextuple dot system. The relation between these two operators is given [29] by

$$\rho(t) = \mathrm{tr}_B\left\{\hat{\rho}(t)\right\} \tag{5.8}$$

where tr_B denotes the trace over all bath parameters. The analog relation for the reduced density operator is then

$$\frac{d\rho_I(t)}{dt} = -\frac{i}{\hbar}\mathrm{tr}_B\left\{[H_T(t), \hat{\rho}_I(0)]_-\right\} - \frac{1}{\hbar^2}\int_0^t dt'\mathrm{tr}_B\left\{[H_T(t), [H_T(t'), \hat{\rho}_I(t')]_-]_-\right\} \tag{5.9}$$

The master equation is obtained from this equation by means of a number of approximations, including the weak interaction limit and the Markov approximation.

Weak Interaction Limit and Unperturbed Bath

Assuming that the density matrix at $t = 0$ can be written as a product of the reduced density matrices of the bath and the open sextuple dot system, respectively, leads to the following relation:

$$\hat{\rho}(0) = \hat{\rho}_I(0) = \rho(0) \otimes \rho_B(0) = \rho_I(0) \otimes \rho_B(0) \tag{5.10}$$

As a first-order approximation this kind of decomposition of the total density matrix is assumed to hold for all times, i.e.,

$$\hat{\rho}_I(t) = \rho_I(t) \otimes \rho_B(t) \tag{5.11}$$

This approximation is valid if the coupling to the bath is weak and the leads have internal dynamics that are much faster than the dynamics of the sextuple dot system.

A second approximation is made by assuming that the bath is unperturbed, i.e., it does not change over time. This leads to

$$\rho_B(t) = \rho_B(0) \equiv \rho_B \tag{5.12}$$

These approximations lead to

$$\mathrm{tr}_B \left\{[H_T(t), \hat{\rho}_I(0)]_-\right\} = \mathrm{tr}_B \left\{[H_T(t), \rho_I(0) \otimes \rho_B]_-\right\} = 0 \tag{5.13}$$

and the master equation can be simplified to

$$\frac{d\rho_I(t)}{dt} = -\frac{1}{\hbar^2} \int_0^t dt' \mathrm{tr}_B \left\{[H_T(t), [H_T(t'), \rho_I(t') \otimes \rho_B]_-]_-\right\} \tag{5.14}$$

Markov Approximation

If the correlation times of the leads are much shorter than the dynamics of the sextuple dot system, the Markov approximation can be used [28]. This approximation implies that the system is time-local, i.e., it has no "memory" of the past. The integral in Eq. (5.14) can then be simplified. A change of variables is used, where $\tau = t - t'$ is introduced. The integral limits are then extended to $[-\infty, 0]$ and $\rho_I(t-\tau)$ is replaced by $\rho_I(t)$. The master equation becomes

$$\frac{d\rho_I(t)}{dt} = -\frac{1}{\hbar^2} \int_{-\infty}^0 d\tau \mathrm{tr}_B \left\{[H_T(t), [H_T(t-\tau), \rho_I(t) \otimes \rho_B]_-]_-\right\} \tag{5.15}$$

Trace Computation

The last step is to compute the trace of the integrand. First, the commutators can be expanded according to

$$\begin{aligned}
&\mathrm{tr}_B \left\{[H_T(t), [H_T(t-\tau), \rho_I(t) \otimes \rho_B]_-]_-\right\} = \\
&\qquad = \mathrm{tr}_B \left\{H_T(t) H_T(t-\tau) \rho_I(t) \otimes \rho_B\right\} - \mathrm{tr}_B \left\{H_T(t-\tau) \rho_I(t) \otimes \rho_B H_T(t)\right\} \\
&\qquad - \mathrm{tr}_B \left\{H_T(t) \rho_I(t) \otimes \rho_B H_T(t-\tau)\right\} + \mathrm{tr}_B \left\{\rho_I(t) \otimes \rho_B H_T(t-\tau) H_T(t)\right\}
\end{aligned} \tag{5.16}$$

The remaining part consists of computing the four traces. In the following the first trace is computed and the other three can be determined analogously. If the leads are in thermal equilibrium with a temperature T and at voltages V_α, the density operator of the bath is explicitly given [26] by

$$\rho_B = \prod_{k\alpha} \Big(f_\alpha(\epsilon_{k\alpha}) c_{k\alpha}^\dagger |0\rangle\langle 0| c_{k\alpha} + (1 - f_\alpha(\epsilon_{k\alpha}))|0\rangle\langle 0| \Big) \tag{5.17}$$

where f_α denotes the Fermi-Dirac distribution function and $|0\rangle$ is the vacuum state.

The expression for the bath density operator makes it possible to evaluate the following traces:

$$\mathrm{tr}_B\big\{ c_{k\alpha} c_{k'\alpha'} \rho_B \big\} = \mathrm{tr}_B\big\{ c_{k\alpha}^\dagger c_{k'\alpha'}^\dagger \rho_B \big\} = 0 \tag{5.18}$$

$$\mathrm{tr}_B\big\{ c_{k\alpha}^\dagger c_{k'\alpha'} \rho_B \big\} = f_\alpha(\epsilon_{k\alpha}) \delta_{kk'} \delta_{\alpha\alpha'} \tag{5.19}$$

$$\mathrm{tr}_B\big\{ c_{k\alpha} c_{k'\alpha'}^\dagger \rho_B \big\} = (1 - f_\alpha(\epsilon_{k\alpha})) \delta_{kk'} \delta_{\alpha\alpha'} \tag{5.20}$$

In the interaction picture, the tunneling Hamiltonian is given by

$$H_T(t) = e^{i(H_S+H_B)t/\hbar} H_T e^{-i(H_S+H_B)t/\hbar} = e^{i(H_S+H_B)t/\hbar} t_{k\alpha} c_{k\alpha}^\dagger d_\alpha e^{-i(H_S+H_B)t/\hbar} + h.c. \tag{5.21}$$

As mentioned in Sec. 3.2, operators acting on different spaces are commuting. Hence, the expression for the tunneling Hamiltonian can be recast into

$$H_T(t) = \sum_{k\alpha} t_{k\alpha} e^{iH_B t/\hbar} c_{k\alpha}^\dagger e^{-iH_B t/\hbar} e^{iH_S t/\hbar} d_\alpha e^{-iH_S t/\hbar} + h.c. \tag{5.22}$$

Using the fact that H_B is diagonal in the basis $\{|k,\alpha\rangle\}$, this part can be rewritten as

$$e^{iH_B t/\hbar} c_{k\alpha}^\dagger e^{-iH_B t/\hbar} = c_{k\alpha}^\dagger e^{-i\epsilon_{k\alpha} t/\hbar} \tag{5.23}$$

In contrast to H_B, H_S is not diagonal in the local Fock basis. But by introducing a new basis for the one- and two-particle subspaces of S, the operator can be rewritten in a diagonal form as

$$H_S = \sum_{\gamma_2} \epsilon_{\gamma_2} |\gamma_2\rangle\langle\gamma_2| + \sum_{\gamma_1} \epsilon_{\gamma_1} |\gamma_1\rangle\langle\gamma_1| + \epsilon_0 |0\rangle\langle 0| \tag{5.24}$$

where $\{|\gamma_2\rangle\}$ spans the two-particle subspace and $\{|\gamma_1\rangle\}$ spans the one-particle subspace. We express the creation and annihilation operators for the dots in the same basis, for instance:

$$d_\alpha = \sum_{\beta_1\beta_2} s_{\alpha\beta_1\beta_2}|\beta_1\rangle\langle\beta_2| + \sum_{\delta_0\delta_1} s_{\alpha\delta_0\delta_1}|\delta_0\rangle\langle\delta_1| \tag{5.25}$$

Hence, the following relation holds:

$$\begin{aligned} e^{iH_S t/\hbar} d_\alpha e^{-iH_S t/\hbar} &= \sum_{\beta_1\beta_2} s_{\alpha\beta_1\beta_2} e^{iH_S t/\hbar}|\beta_1\rangle\langle\beta_2|e^{-iH_S t/\hbar} + \sum_{\delta_0\delta_1} s_{\alpha\delta_0\delta_1} e^{iH_S t/\hbar}|\delta_0\rangle\langle\delta_1|e^{-iH_S t/\hbar} = \\ &= \sum_{\beta_1\beta_2} s_{\alpha\beta_1\beta_2}|\beta_1\rangle\langle\beta_2|e^{i(\epsilon_{\beta_1}-\epsilon_{\beta_2})t/\hbar} + \sum_{\delta_0\delta_1} s_{\alpha\delta_0\delta_1}|\delta_0\rangle\langle\delta_1|e^{i(\epsilon_{\delta_0}-\epsilon_{\delta_1})t/\hbar} \end{aligned} \tag{5.26}$$

For simplicity, we rewrite this in a more compact form:

$$e^{iH_S t/\hbar} d_\alpha e^{-iH_S t/\hbar} = \sum_{\gamma\gamma'} s_{\alpha\gamma\gamma'}|\gamma\rangle\langle\gamma'|e^{i\epsilon_{\gamma\gamma'}t/\hbar} \tag{5.27}$$

Using Eq. (5.23) and Eq. (5.27), Eq. (5.22) can be rewritten as

$$H_T(t) = \sum_{k\alpha\gamma\gamma'} t_{k\alpha} c^\dagger_{k\alpha} e^{-i\epsilon_{k\alpha}t/\hbar} s_{\alpha\gamma\gamma'}|\gamma\rangle\langle\gamma'|e^{i\epsilon_{\gamma\gamma'}t/\hbar} + h.c. \tag{5.28}$$

The trace can now be expressed as

$$\begin{aligned} &\mathrm{tr}_B\left\{H_T(t)H_T(t-\tau)\rho_I(t)\otimes\rho_B\right\} = \\ &\quad= \sum_{k\alpha\gamma\gamma'} t_{k\alpha} e^{-i\epsilon_{k\alpha}t/\hbar} s_{\alpha\gamma\gamma'}|\gamma\rangle\langle\gamma'|e^{i\epsilon_{\gamma\gamma'}t/\hbar} \\ &\qquad\qquad \times \sum_{\delta\delta'} t^*_{k\alpha} e^{i\epsilon_{k\alpha}(t-\tau)/\hbar} s^*_{\alpha\delta\delta'}|\delta'\rangle\langle\delta|e^{-i\epsilon_{\delta\delta'}(t-\tau)/\hbar}\rho_I(t)\mathrm{tr}_B\left\{c^\dagger_{k\alpha}c_{k\alpha}\rho_B\right\} \\ &\quad+ \sum_{k\alpha\gamma\gamma'} t^*_{k\alpha} e^{i\epsilon_{k\alpha}t/\hbar} s^*_{\alpha\gamma\gamma'}|\gamma'\rangle\langle\gamma|e^{-i\epsilon_{\gamma\gamma'}t/\hbar} \\ &\qquad\qquad \times \sum_{\delta\delta'} t_{k\alpha} e^{-i\epsilon_{k\alpha}(t-\tau)/\hbar} s_{\alpha\delta\delta'}|\delta\rangle\langle\delta'|e^{i\epsilon_{\delta\delta'}(t-\tau)/\hbar}\rho_I(t)\mathrm{tr}_B\left\{c_{k\alpha}c^\dagger_{k\alpha}\rho_B\right\} = \\ &= \sum_{\alpha\gamma\gamma'} s_{\alpha\gamma\gamma'}|\gamma\rangle\langle\gamma'|e^{i\epsilon_{\gamma\gamma'}t/\hbar}\sum_{\delta\delta'} s^*_{\alpha\delta\delta'}|\delta'\rangle\langle\delta|e^{-i\epsilon_{\delta\delta'}(t-\tau)/\hbar}\rho_I(t)\sum_k |t_{k\alpha}|^2 f_\alpha(\epsilon_{k\alpha})e^{-i\epsilon_{k\alpha}\tau/\hbar} \\ &\quad+ \sum_{\alpha\gamma\gamma'} s^*_{\alpha\gamma\gamma'}|\gamma'\rangle\langle\gamma|e^{-i\epsilon_{\gamma\gamma'}t/\hbar}\sum_{\delta\delta'} s_{\alpha\delta\delta'}|\delta\rangle\langle\delta'|e^{i\epsilon_{\delta\delta'}(t-\tau)/\hbar}\rho_I(t)\sum_k |t_{k\alpha}|^2(1-f_\alpha(\epsilon_{k\alpha}))e^{i\epsilon_{k\alpha}\tau/\hbar} \end{aligned} \tag{5.29}$$

The other traces are obtained analogously. If the high bias regime is valid, the Fermi functions will be more or less constant in the energy range of interest. Hence, the energy argument can be neglected in the functions, i.e., $f_\alpha(\epsilon_{k\alpha})$ is replaced by f_α. The rates Γ_α at which the electrons tunnel between a dot α and its lead are introduced and defined by

$$\begin{aligned}\Gamma_\alpha f_\alpha &= \frac{2\pi}{\hbar}\sum_k |t_{k\alpha}|^2 f_\alpha(\epsilon_{k\alpha})\delta(\epsilon_{k\alpha}-\epsilon_{\delta\delta'})\\ \Gamma_\alpha(1-f_\alpha) &= \frac{2\pi}{\hbar}\sum_k |t_{k\alpha}|^2 (1-f_\alpha(\epsilon_{k\alpha}))\delta(\epsilon_{k\alpha}-\epsilon_{\delta\delta'})\end{aligned} \tag{5.30}$$

where δ denotes the Dirac delta function. Integration of the first trace part of the integrand yields the following result:

$$\begin{aligned}
&-\frac{1}{\hbar^2}\int_{-\infty}^{0} d\tau \mathrm{tr}_B\left\{H_T(t)H_T(t-\tau)\rho_I(t)\otimes\rho_B\right\} = \\
&\quad = -\frac{1}{\hbar^2}\Bigg(\sum_{\alpha\gamma\gamma'} s_{\alpha\gamma\gamma'}|\gamma\rangle\langle\gamma'|e^{i\epsilon_{\gamma\gamma'}t/\hbar}\sum_{\delta\delta'} s^*_{\alpha\delta\delta'}|\delta'\rangle\langle\delta|e^{-i\epsilon_{\delta\delta'}t/\hbar} \\
&\qquad\qquad \times \rho_I(t)\hbar\pi\sum_k |t_{k\alpha}|^2 f_\alpha(\epsilon_{k\alpha})\delta(\epsilon_{k\alpha}-\epsilon_{\delta\delta'}) \\
&\qquad + \sum_{\alpha\gamma\gamma'} s^*_{\alpha\gamma\gamma'}|\gamma'\rangle\langle\gamma|e^{-i\epsilon_{\gamma\gamma'}t/\hbar}\sum_{\delta\delta'} s_{\alpha\delta\delta'}|\delta\rangle\langle\delta'|e^{i\epsilon_{\delta\delta'}t/\hbar} \\
&\qquad\qquad \times \rho_I(t)\hbar\pi\sum_k |t_{k\alpha}|^2 (1-f_\alpha(\epsilon_{k\alpha}))\delta(\epsilon_{k\alpha}-\epsilon_{\delta\delta'})\Bigg) = \\
&\quad = -\Bigg(\sum_{\alpha\gamma\gamma'} s_{\alpha\gamma\gamma'}|\gamma\rangle\langle\gamma'|e^{i\epsilon_{\gamma\gamma'}t/\hbar}\sum_{\delta\delta'} s^*_{\alpha\delta\delta'}|\delta'\rangle\langle\delta|e^{-i\epsilon_{\delta\delta'}t/\hbar}\rho_I(t)\frac{\Gamma_\alpha}{2}f_\alpha \\
&\qquad + \sum_{\alpha\gamma\gamma'} s^*_{\alpha\gamma\gamma'}|\gamma'\rangle\langle\gamma|e^{-i\epsilon_{\gamma\gamma'}t/\hbar}\sum_{\delta\delta'} s_{\alpha\delta\delta'}|\delta\rangle\langle\delta'|e^{i\epsilon_{\delta\delta'}t/\hbar}\rho_I(t)\frac{\Gamma_\alpha}{2}(1-f_\alpha)\Bigg) = \\
&= -\Bigg(\sum_\alpha e^{iH_S t/\hbar}d_{k\alpha}e^{-iH_S t/\hbar}e^{iH_S t/\hbar}d^\dagger_{k\alpha}e^{-iH_S t/\hbar}\rho_I(t)\frac{\Gamma_\alpha}{2}f_\alpha \\
&\qquad\qquad + \sum_\alpha e^{iH_S t/\hbar}d^\dagger_\alpha e^{-iH_S t/\hbar}e^{iH_S t/\hbar}d_\alpha e^{-iH_S t/\hbar}\rho_I(t)\frac{\Gamma_\alpha}{2}(1-f_\alpha)\Bigg) =
\end{aligned}$$

$$= -e^{iH_S t/\hbar} \sum_\alpha \frac{\Gamma_\alpha}{2} \Big(d_\alpha d_\alpha^\dagger \rho_I(t) f_\alpha + d_\alpha^\dagger d_\alpha \rho_I(t)(1-f_\alpha) \Big) e^{-iH_S t/\hbar}$$

Here we do not explicitly write out the renormalization constant that appears due to the principal value of the integral of the complex exponential function in full. This constant can be taken into account by shifting the energy levels.

Master Equation of the Sextuple Dot System

The other trace parts are given by analog expressions. Taken together, they yield the following result:

$$\frac{d\rho_I(t)}{dt} = -e^{iH_S t/\hbar} \sum_\alpha \frac{\Gamma_\alpha}{2} \Big(\big(d_\alpha d_\alpha^\dagger \rho(t) + \rho(t) d_\alpha d_\alpha^\dagger \big) f_\alpha + \big(d_\alpha^\dagger d_\alpha \rho(t) + \rho(t) d_\alpha^\dagger d_\alpha \big) \big(1 - f_\alpha\big) - 2 d_\alpha^\dagger \rho(t) d_\alpha f_\alpha - 2 d_\alpha \rho(t) d_\alpha^\dagger \big(1 - f_\alpha\big) \Big) e^{-iH_S t/\hbar} \quad (5.31)$$

Together with the relation between the Schrödinger picture and the interaction picture given by

$$\frac{d\rho_I(t)}{dt} = e^{iH_S t/\hbar} \left(\frac{d\rho(t)}{dt} + \frac{i}{\hbar} [H_S, \rho(t)]_- \right) e^{-iH_S t/\hbar} \quad (5.32)$$

the final master equation is obtained as

$$\frac{d\rho(t)}{dt} = -\frac{i}{\hbar}[H_S, \rho(t)]_- - \sum_\alpha \frac{\Gamma_\alpha}{2} \Big(\big(d_\alpha d_\alpha^\dagger \rho(t) + \rho(t) d_\alpha d_\alpha^\dagger \big) f_\alpha + \big(d_\alpha^\dagger d_\alpha \rho(t) + \rho(t) d_\alpha^\dagger d_\alpha \big) \big(1 - f_\alpha\big) - 2 d_\alpha^\dagger \rho(t) d_\alpha f_\alpha - 2 d_\alpha \rho(t) d_\alpha^\dagger \big(1 - f_\alpha\big) \Big) \quad (5.33)$$

5.3 Matrix Representation

From linear algebra, it is well-known that every linear operator can be represented by a matrix when a specific basis is given. To do this, we choose a proper basis, i.e., the local

Fock basis. Due to previous assumptions (see Ch. 3 concerning the different time scales) only two electrons at most can be in the system at the same time. Therefore we only need to consider the zero-, one- and two-particle subspaces of the Hilbert space. Furthermore, it is only possible to have the two-particle states $|12\rangle$, $|35\rangle$, $|36\rangle$, $|45\rangle$ and $|46\rangle$, which means that the only non-zero two-particle populations are $\rho_{12,12}$, $\rho_{35,35}$, $\rho_{36,36}$, $\rho_{45,45}$ and $\rho_{46,46}$. The non-zero coherences are $\rho_{12,35}$, $\rho_{12,36}$, $\rho_{12,45}$, $\rho_{12,46}$ and their Hermitian conjugated counterparts because tunneling can only take place between the center dots and the side dots.

We use the following matrix elements to construct the matrix representation of the master equation. The first elements will appear along the diagonal of the matrix. The elements are determined by expanding the density operator in the Fock basis, e.g.,

$$\langle k|d_\alpha^\dagger d_\alpha \rho|k'\rangle = \sum_{qq'} \rho_{qq'} \langle k|d_\alpha^\dagger d_\alpha|q\rangle\langle q'|k'\rangle = \rho_{kk'} \qquad \forall \alpha \in k \tag{5.34}$$

The remaining non-zero diagonal elements are

$$\begin{aligned}
&\langle k|\rho d_\alpha^\dagger d_\alpha|k'\rangle = \rho_{kk'} && \forall \alpha \in k' \\
&\langle k|d_\alpha d_\alpha^\dagger \rho|k'\rangle = \rho_{kk'} && \forall \alpha \notin k \\
&\langle k|\rho d_\alpha d_\alpha^\dagger|k'\rangle = \rho_{kk'} && \forall \alpha \notin k' \\
&\langle k|n_\alpha n_{\alpha'} \rho|k'\rangle = \rho_{kk'} && \forall (\alpha,\alpha') \in k \\
&\langle k|\rho n_\alpha n_{\alpha'}|k'\rangle = \rho_{kk'} && \forall (\alpha,\alpha') \in k'
\end{aligned}$$

The non-zero off-diagonal elements are

$$\begin{aligned}
&\langle k|d_\alpha^\dagger \rho d_\alpha|k'\rangle = \rho_{k-\alpha,k'-\alpha} && \forall \alpha \in k,k' \\
&\langle k|d_\alpha \rho d_\alpha^\dagger|k'\rangle = \rho_{k+\alpha,k'+\alpha} && \forall \alpha \notin k,k' \\
&\langle k|d_\alpha^\dagger d_{\alpha'}^\dagger d_\beta d_{\beta'} \rho|k'\rangle = \rho_{k,k'-\beta-\beta'+\alpha+\alpha'} && \forall (\beta,\beta') \in k', (\alpha,\alpha') \notin k' \\
&\langle k|\rho d_\alpha^\dagger d_{\alpha'}^\dagger d_\beta d_{\beta'}|k'\rangle = \rho_{k-\beta-\beta'+\alpha+\alpha',k'} && \forall (\beta,\beta') \in k, (\alpha,\alpha') \notin k
\end{aligned}$$

Using these matrix elements and assuming the high bias regime (i.e., $f_1 = f_2 = 1$ and $f_3 = f_4 = f_5 = f_6 = 0$) one obtains the following matrix representation of the master equation:

$$\frac{d\rho}{dt} = M\rho \tag{5.35}$$

where

$$\rho = \begin{pmatrix} \rho_{0,0} \\ \rho_{1,1} \\ \rho_{2,2} \\ \rho_{3,3} \\ \rho_{4,4} \\ \rho_{5,5} \\ \rho_{6,6} \\ \rho_{12,12} \\ \rho_{35,35} \\ \rho_{36,36} \\ \rho_{45,45} \\ \rho_{46,46} \\ \rho_{12,35} \\ \rho_{12,36} \\ \rho_{12,45} \\ \rho_{12,46} \\ \rho^*_{12,35} \\ \rho^*_{12,36} \\ \rho^*_{12,45} \\ \rho^*_{12,46} \end{pmatrix} \tag{5.36}$$

and

$$M = \begin{pmatrix} M_{dd} & \frac{i}{\hbar} M_{dc} \\ \frac{i}{\hbar} M^\dagger_{dc} & M_{cc} \end{pmatrix} \tag{5.37}$$

where

$$M_{dd} =$$

$$\begin{pmatrix}
-\Gamma_1-\Gamma_2 & 0 & 0 & \Gamma_3 & \Gamma_4 & \Gamma_5 & \Gamma_6 & 0 & 0 & 0 & 0 & 0 \\
\Gamma_1 & -\Gamma_2 & 0 & 0 & 0 & 0 & 0 & 0 & 0 & 0 & 0 & 0 \\
\Gamma_2 & 0 & -\Gamma_1 & 0 & 0 & 0 & 0 & 0 & 0 & 0 & 0 & 0 \\
0 & 0 & 0 & -\Gamma_3 & 0 & 0 & 0 & 0 & \Gamma_5 & \Gamma_6 & 0 & 0 \\
0 & 0 & 0 & 0 & -\Gamma_4 & 0 & 0 & 0 & 0 & 0 & \Gamma_5 & \Gamma_6 \\
0 & 0 & 0 & 0 & 0 & -\Gamma_5 & 0 & 0 & \Gamma_3 & 0 & \Gamma_4 & 0 \\
0 & 0 & 0 & 0 & 0 & 0 & -\Gamma_6 & 0 & 0 & \Gamma_3 & 0 & \Gamma_4 \\
0 & \Gamma_2 & \Gamma_1 & 0 & 0 & 0 & 0 & 0 & 0 & 0 & 0 & 0 \\
0 & 0 & 0 & 0 & 0 & 0 & 0 & 0 & -\Gamma_3-\Gamma_5 & 0 & 0 & 0 \\
0 & 0 & 0 & 0 & 0 & 0 & 0 & 0 & 0 & -\Gamma_3-\Gamma_6 & 0 & 0 \\
0 & 0 & 0 & 0 & 0 & 0 & 0 & 0 & 0 & 0 & -\Gamma_4-\Gamma_5 & 0 \\
0 & 0 & 0 & 0 & 0 & 0 & 0 & 0 & 0 & 0 & 0 & -\Gamma_4-\Gamma_6
\end{pmatrix}$$

$$M_{dc} =$$

$$\begin{pmatrix}
0 & 0 & 0 & 0 & 0 & 0 & 0 & 0 \\
0 & 0 & 0 & 0 & 0 & 0 & 0 & 0 \\
0 & 0 & 0 & 0 & 0 & 0 & 0 & 0 \\
0 & 0 & 0 & 0 & 0 & 0 & 0 & 0 \\
0 & 0 & 0 & 0 & 0 & 0 & 0 & 0 \\
0 & 0 & 0 & 0 & 0 & 0 & 0 & 0 \\
0 & 0 & 0 & 0 & 0 & 0 & 0 & 0 \\
t^*_{1235} & t^*_{1236} & t^*_{1245} & t^*_{1246} & -t_{1235} & -t_{1236} & -t_{1245} & -t_{1246} \\
-t^*_{1235} & 0 & 0 & 0 & t_{1235} & 0 & 0 & 0 \\
0 & -t^*_{1236} & 0 & 0 & 0 & t_{1236} & 0 & 0 \\
0 & 0 & -t^*_{1245} & 0 & 0 & 0 & t_{1245} & 0 \\
0 & 0 & 0 & -t^*_{1246} & 0 & 0 & 0 & t_{1246}
\end{pmatrix}$$

$$M_{cc} =$$

$$\begin{pmatrix} c(1235,+) & 0 & 0 & 0 & 0 & 0 & 0 & 0 \\ 0 & c(1236,+) & 0 & 0 & 0 & 0 & 0 & 0 \\ 0 & 0 & c(1245,+) & 0 & 0 & 0 & 0 & 0 \\ 0 & 0 & 0 & c(1246,+) & 0 & 0 & 0 & 0 \\ 0 & 0 & 0 & 0 & c(1235,-) & 0 & 0 & 0 \\ 0 & 0 & 0 & 0 & 0 & c(1236,-) & 0 & 0 \\ 0 & 0 & 0 & 0 & 0 & 0 & c(1245,-) & 0 \\ 0 & 0 & 0 & 0 & 0 & 0 & 0 & c(1246,-) \end{pmatrix}$$

with

$$c(12xy,\pm) = -\Gamma_x/2 - \Gamma_y/2 \pm \frac{i}{\hbar}\epsilon_{12xy}$$

where the co-tunneling energy differences are given by

$$\epsilon_{12xy} = \epsilon_x + \epsilon_y + U_{xy} - \epsilon_1 - \epsilon_2 - U_{12}$$

If the co-tunneling is at resonance, we get $\epsilon_{12xy} = 0$. Note that all parameters are the renormalized ones from the Schrieffer-Wolff transformation.

The eigenvalues and eigenstates of M are important since they describe the time evolution of the system. The steady-state is given as the eigenstate with an eigenvalue equal to zero. The general solution to the master equation in Eq. (5.35) is given by an exponential matrix function. After a sufficiently long time, the transients of all non-zero eigenvalues will have declined and the only surviving eigenstate is the one belonging to the eigenvalue equal to zero. This means that the state approaches the steady-state when a sufficiently long time has elapsed.

Chapter 6

Full Counting Statistics

Like many other concepts in solid-state physics, full counting statistics (FCS) originates from quantum optics [30, 31] and was originally used for studying photons. During the 1990s, FCS started to become an important tool for studying electron transport as well [32, 33]. Since 2003, FCS has been used for studying systems governed by master equations [34]. Flindt et al. used FCS for nano-electromechanical systems in 2005, using a Markovian master equation [35]. In 2006, Kießlich et al. used the concept to study two coupled quantum dots with coherences [36].

The FCS can be used to characterize the currents and noise of the electron transport in the sextuple dot system using the so-called cumulant generating function (CGF). This concept is further discussed in Sec. 6.1 and applied to the sextuple dot system in Sec. 6.2. In the latter section, the master equation from Ch. 5 is used to compute the CGF of the sextuple dot system, which is the main result of this chapter.

6.1 Counting Fields

A central concept related to FCS is the probability distribution $P_\tau(N)$, which describes the probability that a number of electrons N has passed through a conductor, e.g., a quantum dot, during a long measurement time τ (relative to the dynamics). The CGF is then given [37] by

$$F(\chi) = \ln\left[\sum_{N=-\infty}^{\infty} e^{iN\chi} P_\tau(N)\right] \tag{6.1}$$

where the *counting field* χ has been introduced. Note that the relation between $e^{F(\chi)}$ and

$P_\tau(N)$ is given by a (discrete) Fourier transform, where the counting field χ is the conjugated variable to the number of electrons N.

Instead of considering the distribution $P_\tau(N)$, we can study the CGF. The advantage of using the CGF is that it has a simple physical interpretation. From the function we get the cumulants that correspond to different properties of the current. The n:th cumulant is mathematically obtained from $F(\chi)$ by

$$\kappa_n = \frac{\partial^n}{\partial(i\chi)^n} F(\chi)\bigg|_{\chi=0} \tag{6.2}$$

The first cumulant corresponds to the average current, the second cumulant to the variance and the third cumulant to the skewness. Higher-order cumulants describe other statistical quantitites [38].

Returning to the master equation, we can keep track of the electrons in the different dots by using the counting fields. In the case of the sextuple dot system, we have six different dots and therefore we have to use six counting fields, one for each dot. The previous theory consequently has to be extended to several dimensions. The counting field $\chi = (\chi_1, \chi_2, \chi_3, \chi_4, \chi_5, \chi_6)$ becomes a vector. They are added as exponentials in the form $e^{i\chi_N}$ and $e^{-i\chi_N}$ in the matrix elements of M_{dd} corresponding to an electron jumping into the sextuple dot system and an electron jumping out of the sextuple dot system, respectively. We then obtain the following matrix representation:

$$M_{dd}(\chi) = \tag{6.3}$$

$$\begin{pmatrix}
-\Gamma_1-\Gamma_2 & 0 & 0 & \Gamma_3 e^{i\chi_3} & \Gamma_4 e^{i\chi_4} & \Gamma_5 e^{i\chi_5} & \Gamma_6 e^{i\chi_6} & 0 & 0 & 0 & 0 & 0 \\
\Gamma_1 e^{-i\chi_1} & -\Gamma_2 & 0 & 0 & 0 & 0 & 0 & 0 & 0 & 0 & 0 & 0 \\
\Gamma_2 e^{-i\chi_2} & 0 & -\Gamma_1 & 0 & 0 & 0 & 0 & 0 & 0 & 0 & 0 & 0 \\
0 & 0 & 0 & -\Gamma_3 & 0 & 0 & 0 & 0 & \Gamma_5 e^{i\chi_5} & \Gamma_6 e^{i\chi_6} & 0 & 0 \\
0 & 0 & 0 & 0 & -\Gamma_4 & 0 & 0 & 0 & 0 & 0 & \Gamma_5 e^{i\chi_5} & \Gamma_6 e^{i\chi_6} \\
0 & 0 & 0 & 0 & 0 & -\Gamma_5 & 0 & 0 & \Gamma_3 e^{i\chi_3} & 0 & \Gamma_4 e^{i\chi_4} & 0 \\
0 & 0 & 0 & 0 & 0 & 0 & -\Gamma_6 & 0 & 0 & \Gamma_3 e^{i\chi_3} & 0 & \Gamma_4 e^{i\chi_4} \\
0 & \Gamma_2 e^{-i\chi_2} & \Gamma_1 e^{-i\chi_1} & 0 & 0 & 0 & 0 & 0 & 0 & 0 & 0 & 0 \\
0 & 0 & 0 & 0 & 0 & 0 & 0 & 0 & -\Gamma_3-\Gamma_5 & 0 & 0 & 0 \\
0 & 0 & 0 & 0 & 0 & 0 & 0 & 0 & 0 & -\Gamma_3-\Gamma_6 & 0 & 0 \\
0 & 0 & 0 & 0 & 0 & 0 & 0 & 0 & 0 & 0 & -\Gamma_4-\Gamma_5 & 0 \\
0 & 0 & 0 & 0 & 0 & 0 & 0 & 0 & 0 & 0 & 0 & -\Gamma_4\Gamma_6
\end{pmatrix}$$

where Γ_α still denotes the rate at which electrons tunnel between dot α and its lead.

The CGF can now be obtained from the master equation as the eigenvalue $F(\chi)$ of $M(\chi)$ in Eq. (5.35) that fulfills the condition $\lim_{\chi \to 0} F(\chi) = 0$. This eigenvalue corresponds to the stationary eigenstate and will be computed in the next section.

6.2 Cumulant Generating Function

The CGF is given as an eigenvalue of $M(\chi)$. The eigenvalue problem reads as

$$M(\chi)\rho_{stat}(\chi) = F(\chi)\rho_{stat}(\chi) \tag{6.4}$$

where ρ_{stat} is the stationary density operator. The dimension of $M(\chi)$ is too large to directly compute the eigenvalues analytically. Therefore several approximations have to be used.

First we write ρ_{stat} as a vector in the form $\begin{pmatrix} \rho_d \\ \rho_c \end{pmatrix}$, where ρ_d includes the populations and ρ_c the coherences of ρ_{stat}. The eigenvalue problem can then be written as the following system of equations:

$$\begin{aligned} M_{dd}\rho_d + M_{dc}\rho_c &= F(\chi)\rho_d \\ M_{cd}\rho_d + M_{cc}\rho_c &= F(\chi)\rho_c \end{aligned} \tag{6.5}$$

The second equation can be rewritten as

$$\rho_c = (F(\chi) - M_{cc})^{-1} M_{cd}\rho_d \tag{6.6}$$

$F(\chi)$ can be expanded in terms of the co-tunneling amplitudes $t_{\alpha\alpha'\beta\beta'}$. Since these are small compared to the elements of M_{cc}, we get

$$\rho_c = -M_{cc}^{-1} M_{cd}\rho_d \tag{6.7}$$

Inserting this back into the first equation yields

$$M_{dd}\rho_d - M_{dc}M_{cc}^{-1}M_{cd}\rho_d = F(\chi)\rho_d \tag{6.8}$$

Hence, $F(\chi)$ can be obtained as the eigenvalue of $M_{red} = M_{dd} - M_{dc}M_{cc}^{-1}M_{cd}$, which is of a lower matrix dimension than M. The lower dimension requires less computational power. M_{red} is given by

$$M_{red}(\chi) = \tag{6.9}$$

$$\begin{pmatrix}
-\Gamma_1-\Gamma_2 & 0 & 0 & \Gamma_3 e^{i\chi_3} & \Gamma_4 e^{i\chi_4} & \Gamma_5 e^{i\chi_5} & \Gamma_6 e^{i\chi_6} & 0 & 0 & 0 & 0 & 0 \\
\Gamma_1 e^{-i\chi_1} & -\Gamma_2 & 0 & 0 & 0 & 0 & 0 & 0 & 0 & 0 & 0 & 0 \\
\Gamma_2 e^{-i\chi_2} & 0 & -\Gamma_1 & 0 & 0 & 0 & 0 & 0 & 0 & 0 & 0 & 0 \\
0 & 0 & 0 & -\Gamma_3 & 0 & 0 & 0 & 0 & \Gamma_5 e^{i\chi_5} & \Gamma_6 e^{i\chi_6} & 0 & 0 \\
0 & 0 & 0 & 0 & -\Gamma_4 & 0 & 0 & 0 & 0 & 0 & \Gamma_5 e^{i\chi_5} & \Gamma_6 e^{i\chi_6} \\
0 & 0 & 0 & 0 & 0 & -\Gamma_5 & 0 & 0 & \Gamma_3 e^{i\chi_3} & 0 & \Gamma_4 e^{i\chi_4} & 0 \\
0 & 0 & 0 & 0 & 0 & 0 & -\Gamma_6 & 0 & 0 & \Gamma_3 e^{i\chi_3} & 0 & \Gamma_4 e^{i\chi_4} \\
0 & \Gamma_2 e^{-i\chi_2} & \Gamma_1 e^{-i\chi_1} & 0 & 0 & 0 & 0 & -\sum_{xy} a_{xy} & a_{35} & a_{36} & a_{45} & a_{46} \\
0 & 0 & 0 & 0 & 0 & 0 & 0 & a_{35} & -\Gamma_3-\Gamma_5-a_{35} & 0 & 0 & 0 \\
0 & 0 & 0 & 0 & 0 & 0 & 0 & a_{36} & 0 & -\Gamma_3-\Gamma_6-a_{36} & 0 & 0 \\
0 & 0 & 0 & 0 & 0 & 0 & 0 & a_{45} & 0 & 0 & -\Gamma_4-\Gamma_5-a_{45} & 0 \\
0 & 0 & 0 & 0 & 0 & 0 & 0 & a_{46} & 0 & 0 & 0 & -\Gamma_4-\Gamma_6-a_{46}
\end{pmatrix}$$

where the co-tunneling rates between the center dots and each pair of a left side dot x and a right side dot y are given by

$$a_{xy} = \frac{|t_{12xy}|^2(\Gamma_x + \Gamma_y)}{\hbar^2(\frac{\Gamma_x}{2} + \frac{\Gamma_y}{2})^2 + \epsilon_{12xy}^2} \tag{6.10}$$

where the co-tunneling energy differences are given by $\epsilon_{12xy} = \epsilon_x + \epsilon_y + U_{xy} - \epsilon_1 - \epsilon_2 - U_{12}$. If the co-tunneling is at resonance, we get $\epsilon_{12xy} = 0$. By writing M_{red} in the form

$$M_{red} = \begin{pmatrix} M_{00} & A \\ B & C \end{pmatrix} \tag{6.11}$$

where M_{00} corresponds to the zero-particle subspace, the eigenvalue is obtained from

$$\det \begin{pmatrix} M_{00} - F(\chi) & A \\ B & C - F(\chi) \end{pmatrix} = \det\Big(D\Big)\det\Big(\big(M_{00} - F(\chi)\big) - AD(\chi)^{-1}B\Big) = 0 \tag{6.12}$$

where $D(\chi) = C - F(\chi)$. Since $\det(D) \neq 0$, this implies $(M_{00} - F(\chi)) - AD(\chi)^{-1}B = 0$. This equation can be solved to first order in the co-tunneling rates a_{xy}.

The CGF can finally be obtained as

$$F(\chi) = \sum_{xy} (e^{i(\chi_x + \chi_y - \chi_1 - \chi_2)} - 1) a_{xy} \tag{6.13}$$

where $x \in \{3, 4\}$ denotes any of the left side dots and $y \in \{5, 6\}$ denotes any of the right side dots.

Eq. (6.13) has a clear physical interpretation that describes the charge transfer of the sextuple dot system. Each of the four terms in the sum corresponds to one of the co-tunneling processes. The exponent $(e^{i(\chi_x + \chi_y - \chi_1 - \chi_2)} - 1)$ tells us that two electrons are moved from the center dots to the left side dot x and the right side dot y. Subsequent co-tunneling processes are uncorrelated, so the electrons are Poisson distributed. The processes happen at a rate given by the co-tunneling rates a_{xy}. The rates Γ_α do not appear in the CGF since the transport is limited by the weak co-tunneling rates, and not by the rates between the dots and the leads.

The co-tunneling rates a_{xy} are given by the cross-correlations between an electron entering dot x and another electron entering dot y. This can be shown mathematically by differentiating the CGF with respect to different counting fields:

$$\left.\frac{\partial^2 F(\chi)}{\partial(i\chi_x)\partial(i\chi_y)}\right|_{\chi=0} = a_{xy} \tag{6.14}$$

It is natural to interpret the co-tunneling rates a_{xy} as the analogs to the probabilities used for the formulation of the quantum correlation given by Eq. (2.2). In the next chapter, this interpretation will be used to formulate Bell's inequality.

Chapter 7

Bell's Inequality

In this chapter, Bell's inequality is derived for the sextuple dot system using the generalized version of CHSH [14], which was introduced in Sec. 2.2. It is shown that quantum correlations between charge transport through the side dots will violate the inequality and thereby local realism. We express these quantum correlations in terms of the co-tunneling rates a_{xy} in accordance with the interpretation in the previous chapter. These rates can be measured experimentally since they correspond to the cross-correlations of the currents. In Sec. 7.4, we also investigate short-time measurements by using the concept of second degree of coherence.

7.1 Simplifying Assumptions

In the following, the co-tunneling processes will be assumed to be at resonance. This means that $\epsilon_{12xy} = \epsilon_x + \epsilon_y + U_{xy} - \epsilon_1 - \epsilon_2 - U_{12} = 0$ in Eq. (6.10) for all values of x and y. Furthermore, due to symmetry on each side of the center dots, $\Gamma_x = \Gamma_L$ and $\Gamma_y = \Gamma_R$ are assumed to be the same for the dot pairs on each side. Consequently, the co-tunneling rates from Eq. (6.10) become

$$a_{xy} = \frac{|t_{12xy}|^2(\Gamma_L + \Gamma_R)}{\hbar^2(\frac{\Gamma_L}{2} + \frac{\Gamma_R}{2})^2} \propto |t_{12xy}|^2 \tag{7.1}$$

7.2 CHSH Inequality

The CHSH inequality can be formulated by introducing the quantum correlation

$$E = \frac{a_{35} + a_{46} - a_{36} - a_{45}}{a_{35} + a_{46} + a_{36} + a_{45}} \tag{7.2}$$

Since the co-tunneling rates a_{xy} all depend on the tunneling amplitudes, E will depend on the tunneling amplitudes as well. Bell's inequality is obtained by performing four different experiments, each with a unique setup of tunneling amplitudes. Hence, four different quantum correlations will be obtained.

First, a reference measurement is performed with the quantum correlation E_{ab}. Then the circumstances are changed such that the tunneling amplitudes between the center dots and the left side dots are changed, yielding a quantum correlation $E_{a'b}$. In the third experiment, the circumstances for the left side dots are the same as in the reference experiment, but now the circumstances are changed for the right side dots, yielding a quantum correlation $E_{ab'}$. Finally, a fourth measurement is performed where the circumstances are changed for both the left side dots and the right side dots at the same time, yielding a quantum correlation $E_{a'b'}$.

The Bell parameter is then defined by

$$S = |E_{ab} - E_{a'b} + E_{ab'} + E_{a'b'}| \tag{7.3}$$

where local realism implies that this parameter never exceeds a maximum value of 2. By showing that four experiments can violate this inequality, one can demonstrate the effect of entanglement. Since the inequality is not violated by every choice of four different experiments, the challenge is to find four experiments that violate the inequality.

7.3 Parameterization of the Tunneling Amplitudes

To explicitly show that the system violates Bell's inequality, we parameterize the tunneling amplitudes. We assume that the tunneling amplitudes between the center dots and the side dots can be tuned by changing the potential of some electrode. Furtermore, we assume that this is mathematically analogous to a beam splitter in quantum optics. This means that the tunneling amplitudes can be parameterized as shown in Fig. 7.1. It follows that

$$\begin{aligned}
t_{1235} &= b(t_{13}t_{25} - t_{15}t_{23}) = b(\sin\theta_1\cos\theta_2 - \sin\theta_2\cos\theta_1) = b\sin(\theta_1 - \theta_2) \\
t_{1236} &= b(t_{13}t_{26} - t_{16}t_{23}) = b(-\sin\theta_1\sin\theta_2 - \sin\theta_2\sin\theta_1) = -b\cos(\theta_1 - \theta_2) \\
t_{1245} &= b(t_{14}t_{25} - t_{15}t_{24}) = b(\cos\theta_1\cos\theta_2 + \sin\theta_2\sin\theta_1) = b\cos(\theta_1 - \theta_2) \\
t_{1246} &= b(t_{14}t_{26} - t_{16}t_{24}) = b(-\cos\theta_1\sin\theta_2 + \cos\theta_2\sin\theta_1) = b\sin(\theta_1 - \theta_2)
\end{aligned} \tag{7.4}$$

where b is a proportionality constant. These results give the following expressions for the

co-tunneling rates:

$$\begin{aligned} a_{35} = a_{46} &\propto \sin^2(\theta_1 - \theta_2) \\ a_{36} = a_{45} &\propto \cos^2(\theta_1 - \theta_2) \end{aligned} \tag{7.5}$$

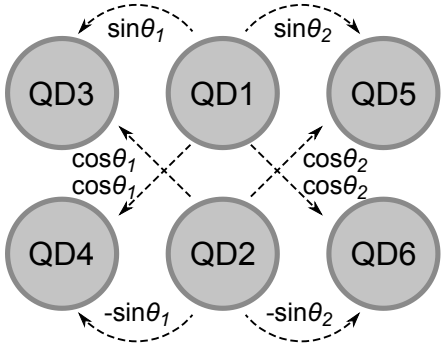

Figure 7.1: The parameterization of the sequential tunneling amplitudes.

For a given setup (θ_1, θ_2), which defines the tunneling amplitudes, the quantum correlation is now explicitly given by

$$E(\theta_1, \theta_2) = \frac{a_{35} + a_{46} - a_{36} - a_{45}}{a_{35} + a_{46} + a_{36} + a_{45}} = -\cos(2(\theta_1 - \theta_2)) \tag{7.6}$$

The Bell parameter in the CHSH inequality becomes then

$$\begin{aligned} S = |E(\theta_1, \theta_2) - E(\theta_1, \theta_2') + E(\theta_1', \theta_2) + E(\theta_1', \theta_2')| = \\ = |-\cos(2(\theta_1 - \theta_2)) + \cos(2(\theta_1 - \theta_2')) - \cos(2(\theta_1' - \theta_2)) - \cos(2(\theta_1' - \theta_2'))| \end{aligned} \tag{7.7}$$

where local realism implies that this parameter never exceeds a maximum value of 2. Nevertheless, by choosing the angles properly (e.g., $\theta_1 = \pi/2$, $\theta_1' = \pi/4$, $\theta_2 = 3\pi/8$ and $\theta_2' = \pi/8$) the expression can achieve values as high as $2\sqrt{2}$ if the predictions of quantum mechanics are correct. We have thus shown that, under certain assumptions, the sextuple dot system displays non-local transport properties.

7.4 Short-Time Measurements

In the previous sections, the quantum correlations were determined based on average currents obtained from the FCS. All these concepts are based on long-time measurements. To really

achieve the analog case of quantum optics, where correlations between measurements on single photons are conducted, we need to consider short-time measurements.

Until recently, it has not been possible to perform such experiments since it requires measurement devices that can detect single electrons. However, during the last years quantum point contacts have been developed that allow for detection of single electrons [39]. This means that short-time measurements analogous to the ones performed in quantum optics can be conducted.

To compute the quantum correlations in the short-time limit, we use the concept of second degree of coherence. This is a concept used in quantum optics to describe correlations between intensity fluctuations [40]. Recently, it has also been applied to solid-state physics [41]. In our case, the second degree of coherence can be defined as

$$g_{xy}^{(2)}(\tau) = \frac{\langle\langle J_x \Omega(\tau) J_y \rangle\rangle + \langle\langle J_y \Omega(\tau) J_x \rangle\rangle}{2\langle\langle J_x \rangle\rangle \langle\langle J_y \rangle\rangle} \tag{7.8}$$

where $\langle\langle A \rangle\rangle = \mathrm{tr}\{A\rho_{stat}\}$ denotes the stationary expectation value of the operator A, $\Omega(\tau) = e^{M\tau}$ is the master equation propagator and $J_N = \frac{\partial}{\partial(i\chi_N)} M(\chi)\big|_{\chi=0}$ is the operator corresponding to the charge flux through side dot N. In the limit when $\tau \to 0$, we get $\Omega(\tau) = 1$. It can easily be shown that J_x and J_y are commuting, i.e., $\langle\langle J_x J_y \rangle\rangle = \langle\langle J_y J_x \rangle\rangle$. Hence, for the sextuple dots, the second degree of coherence becomes to first order in a_{xy}

$$g_{xy}^{(2)}(0) = \frac{\langle\langle J_x J_y \rangle\rangle}{\langle\langle J_x \rangle\rangle \langle\langle J_y \rangle\rangle} = a_{xy} \frac{\Gamma_x \Gamma_y}{\Gamma_x + \Gamma_y} \frac{1}{(a_{xy} + a_{x\bar{y}})(a_{xy} + a_{\bar{x}y})} \tag{7.9}$$

The third factor in this expression is a normalization constant and becomes a fixed number. If we use the previous assumption that $\Gamma_x = \Gamma_L$ and $\Gamma_y = \Gamma_R$ are the same for the dot pairs on each side, the expression simplifies to

$$g_{xy}^{(2)}(0) = a_{xy} \frac{\Gamma_L \Gamma_R}{\Gamma_L + \Gamma_R} \propto a_{xy} \tag{7.10}$$

Interpreting this as the analog to the probabilities used for the formulation of the quantum correlation given by Eq. (2.2), we note that we end up with quantum correlations that are still given by the a_{xy} coefficients. Hence, the results for long-time measurements hold also for short-time measurements.

Chapter 8

Discussion and Conclusion

The aim of this thesis was to present and analyze a sextuple dot system with the purpose to make it possible to experimentally demonstrate entanglement between electrons in nanostructures. As shown in Ch. 4, the system operates in the co-tunneling regime under the given assumptions as intended. In Ch. 5, we derived a master equation and from this we computed the full counting statistics in Ch. 6. By using the a_{xy} co-tunneling rates we obtained expressions for the quantum correlations. The results showed that the system violates Bell's inequality and thus displays quantum coherent non-local transport properties. This phenomenon is a consequence of the actual existence of quantum entanglement between electrons.

In Ch. 7, we also showed that the results hold for short-time measurements. Using the second degree of coherence, we concluded that the quantum correlations will be the same as for the long-time measurements.

The main advantage of this system is the short time between production and detection of the entangled electrons. This minimizes the environment-induced decoherence, which would otherwise impair the entanglement. The system is also based on the use of spatially separated electrons, which are easy to detect. There are no obstacles such as measuring spin along arbitrary directions. Hence, the system combines the simple detection of spatially separated electrons with the good coherence properties that usually only characterize spin-entangled electrons.

Even though the results are promising, there are several challenges associated with the system. The structure consists of six quantum dots, which are coupled in a specific way that may be difficult to realize in practice. It must also be possible to tune the tunneling amplitudes between the center dots and the side dots as required.

Further theoretical work should focus on trying to eliminate some of the assumptions that have been used. For instance, it would be advantageous if the model could take into account

the possibility of having tunneling between the two center dots or between two side dots.

In conclusion, this system opens up a new alternative of how entanglement between spatially separated electrons in nanostructures can be demonstrated. A deeper knowledge and understanding of entanglement is important for further developments in quantum information, including the development of quantum computers.

Chapter A

Appendix: Generator S in Ch. 4

In this appendix, we show that

$$V + [S, H_0]_- = 0 \tag{A.1}$$

where

$$V = \sum_{\alpha\alpha'} \frac{1}{2} \left(t_{\alpha\alpha'} d_\alpha^\dagger d_{\alpha'} + t_{\alpha\alpha'}^* d_{\alpha'}^\dagger d_\alpha \right) \tag{A.2}$$

$$H_0 = \sum_\alpha \epsilon_\alpha n_\alpha + \sum_{\alpha\alpha'} \frac{1}{2} U_{\alpha\alpha'} n_\alpha n_{\alpha'} \tag{A.3}$$

has the solution

$$S = \sum_{\alpha\alpha'} \frac{1}{2} E_{\alpha\alpha'} \left(t_{\alpha\alpha'} d_\alpha^\dagger d_{\alpha'} - t_{\alpha\alpha'}^* d_{\alpha'}^\dagger d_\alpha \right) \tag{A.4}$$

with

$$E_{\alpha\alpha'} = \sum_{B \in \mathbb{B}} \left(\frac{1}{\epsilon_B} \prod_{\beta \in B} n_\beta \prod_{\beta \notin B} (1 - n_\beta) \right) \tag{A.5}$$

where $\mathbb{B}$ is the set of all possible combinations of occupied dot states, except the dot states α and α', and ϵ_B is the energy difference between the final state and the initial state when tunneling takes place between dot α and dot α' with the occupation combination B. Note that $E_{\alpha\alpha'} = -E_{\alpha'\alpha}$ and $E_{\alpha\alpha'}^\dagger = E_{\alpha\alpha'}$.

Since S is anti-Hermitian, we start by writing the generator in the form $S = S' - S'^{\dagger}$, where S' is an arbitrary operator. Eq. (A.1) can then be recast into

$$V + [S, H_0]_- = V' + V'^{\dagger} + [S', H_0]_- + [S', H_0]_-^{\dagger} = 0 \tag{A.6}$$

where $V' = \sum_{\alpha\alpha'} \frac{1}{2} t_{\alpha\alpha'} d_\alpha^\dagger d_{\alpha'}$. By separating non-conjugated parts from conjugated ones, a possible solution is given by

$$V' + [S', H_0]_- = 0 \tag{A.7}$$

Next, we make the assumption that S' can be written in the same form as V', i.e., $S' = \sum_{\alpha\alpha'} S'_{\alpha\alpha'}$, where $S'_{\alpha\alpha'}$ is an operator acting exclusively on dot α and α'. Eq. (A.7) becomes then

$$\sum_{\alpha\alpha'} V'_{\alpha\alpha'} + [\sum_{\alpha\alpha'} S'_{\alpha\alpha'}, H_0]_- = 0 \tag{A.8}$$

Due to the linearity of the commutator, this is equivalent to

$$\sum_{\alpha\alpha'} V'_{\alpha\alpha'} + \sum_{\alpha\alpha'} [S'_{\alpha\alpha'}, H_0]_- = 0 \tag{A.9}$$

A solution can be found by solving the following equation for each pair of dots (actually there are two equations for each pair since the order of the indices matters):

$$V'_{\alpha\alpha'} + [S'_{\alpha\alpha'}, H_0]_- = 0 \qquad \forall(\alpha, \alpha') \tag{A.10}$$

Since H_0 only consists of number operators, $S'_{\alpha\alpha'}$ commutes with all parts of H_0 that act on different states. Hence, Eq. (A.10) can be simplified to

$$\begin{aligned} V'_{\alpha\alpha'} + [S'_{\alpha\alpha'}, H^d_\alpha + H^d_{\alpha'} + \sum_{\substack{\alpha'' \\ \alpha'' \neq \alpha, \alpha'}} (H^{\text{cap}}_{\alpha\alpha''} + H^{\text{cap}}_{\alpha''\alpha} + H^{\text{cap}}_{\alpha'\alpha''} + H^{\text{cap}}_{\alpha''\alpha'}) + H^{\text{cap}}_{\alpha\alpha'} + H^{\text{cap}}_{\alpha'\alpha}]_- = \\ = V'_{\alpha\alpha'} + [S'_{\alpha\alpha'}, H^d_\alpha + H^d_{\alpha'} + \sum_{\substack{\alpha'' \\ \alpha'' \neq \alpha, \alpha'}} (2H^{\text{cap}}_{\alpha\alpha''} + 2H^{\text{cap}}_{\alpha'\alpha''}) + 2H^{\text{cap}}_{\alpha\alpha'}]_- = 0 \quad \forall(\alpha, \alpha') \end{aligned} \tag{A.11}$$

We finally show that

$$S'_{\alpha\alpha'} = \frac{1}{2} t_{\alpha\alpha'} E_{\alpha\alpha'} d_\alpha^\dagger d_{\alpha'} \tag{A.12}$$

with

$$E_{\alpha\alpha'} = \sum_{B\in\mathbb{B}} \left(\frac{1}{\epsilon_B} \prod_{\beta\in B} n_\beta \prod_{\beta\notin B} (1-n_\beta) \right) \tag{A.13}$$

is the solution:

$$\begin{aligned}
&[\frac{1}{2} t_{\alpha\alpha'} E_{\alpha\alpha'} d^\dagger_\alpha d_{\alpha'}, H^d_\alpha + H^d_{\alpha'} + \sum_{\substack{\alpha'' \\ \alpha''\neq\alpha,\alpha'}} (2H^{\rm cap}_{\alpha\alpha''} + 2H^{\rm cap}_{\alpha'\alpha''}) + 2H^{\rm cap}_{\alpha\alpha'}]_- = \\
&\qquad = \frac{1}{2} t_{\alpha\alpha'} E_{\alpha\alpha'} [d^\dagger_\alpha d_{\alpha'}, H^d_\alpha + H^d_{\alpha'} + \sum_{\substack{\alpha'' \\ \alpha''\neq\alpha,\alpha'}} (2H^{\rm cap}_{\alpha\alpha''} + 2H^{\rm cap}_{\alpha'\alpha''}) + 2H^{\rm cap}_{\alpha\alpha'}]_- = \\
&\qquad\qquad = -\frac{1}{2} t_{\alpha\alpha'} \sum_{B\in\mathbb{B}} \left(\prod_{\beta\in B} n_\beta \prod_{\beta\notin B} (1-n_\beta) \right) d^\dagger_\alpha d_{\alpha'} = -\frac{1}{2} t_{\alpha\alpha'} d^\dagger_\alpha d_{\alpha'} = -V'_{\alpha\alpha'}
\end{aligned} \tag{A.14}$$

References

[1] A. Einstein, B. Podolsky, and N. Rosen, Phys. Rev. **47**, 777 (1935).

[2] J. S. Bell, Physics **1**, 195 (1964).

[3] A. Aspect, J. Dalibard, and G. Roger, Phys. Rev. Lett. **49**, 1804 (1982).

[4] G. Weihs, T. Jennewein, C. Simon, H. Weinfurter, and A. Zeilinger, Phys. Rev. Lett. **81**, 5039 (1998).

[5] T. Scheidl, R. Ursin, J. Kofler, S. Ramelow, X.-S. Ma, T. Herbst, L. Ratschbacher, A. Fedrizzi, N. K. Langford, T. Jennewein, et al., Proceedings of the National Academy of Sciences of the United States of America **46**, 19708 (2010).

[6] M. Giustina, A. Mech, S. Ramelow, B. Wittmann, J. Kofler, J. Beyer, A. Lita, B. Calkins, T. Gerrits, S. W. Nam, et al., Nature **497**, 227 (2013).

[7] C. W. J. Beenakker, Proc. Int. School Phys. E. Fermi **162** (2006).

[8] D. Bohm and Y. Aharonov, Phys. Rev. **108**, 1070 (1957).

[9] J. F. Clauser and A. Shimony, Reports on Progress in Physics **41**, 1881 (1978).

[10] J. von Neumann, *Mathematische Grundlagen der Quantenmechanik* (Grundlehren der math. Wissensch. Bd. 38, Springer, Berlin, 1932).

[11] J. S. Bell, Rev. Mod. Phys. **38**, 447 (1966).

[12] D. Bohm, Phys. Rev. **85**, 166 (1952).

[13] D. Bohm, Phys. Rev. **85**, 180 (1952).

[14] J. F. Clauser, M. A. Horne, A. Shimony, and R. A. Holt, Phys. Rev. Lett. **23**, 880 (1969).

[15] S. J. Freedman and J. F. Clauser, Phys. Rev. Lett. **28**, 938 (1972).

[16] H. Bruus and K. Flensberg, *Many-Body Quantum Theory in Condensed Matter Physics* (Oxford Graduate Texts, 2004), p. 1–31.

[17] V. Körting, Ph.D. thesis, Fakultät für Physik der Universität, Karlsruhe (2007), p. 169.

[18] J. Koch, Ph.D. thesis, Institut für Theoretische Physik, Freie Universität Berlin (2006), p. 122.

[19] J. R. Schrieffer and P. A. Wolff, Phys. Rev. **149**, 491 (1966).

[20] V. N. Golovach and D. Loss, Europhys. Lett. **62**, 83 (2003).

[21] V. N. Golovach and D. Loss, Phys. Rev. B **69**, 245327 (2004).

[22] F. W. Jayatilaka, M. R. Galpin, and D. E. Logan, Phys. Rev. B **84**, 115111 (2011).

[23] S. Bravyi, D. P. DiVincenzo, and D. Loss, Ann. Phys. **326** (2011).

[24] M. A. Nielsen and I. L. Chuang, *Quan-*

tum Computation and Quantum Information (Cambridge University Press, 2000), p. 101.

[25] C. Gardiner and P. Zoller, *Quantum Noise: A Handbook of Markovian and Non-Markovian Quantum Stochastic Methods with Applications to Quantum Optics* (Springer, 2004).

[26] P. Samuelsson, *Derivation, Quantum Master Equation* (unpublished).

[27] J. J. Sakurai and J. Napolitano, *Modern Quantum Mechanics* (Pearson Education, 2010), 2nd ed., p. 338.

[28] G. M. Moy, J. J. Hope, and C. M. Savage, Phys. Rev. A **59**, 667 (1999).

[29] M. A. Nielsen and I. L. Chuang, *Quantum Computation and Quantum Information* (Cambridge University Press, 2000), p. 105.

[30] L. Mandel, Optics. Lett. **4**, 205 (1979).

[31] R. J. Cook, Phys. Rev. A **23**, 1243 (1981).

[32] L. S. Levitov, H.-W. Lee, and G. B. Lesovik, J. Math. Phys. **37**, 4845 (1996).

[33] M. Esposito, U. Harbola, and S. Mukamel, Phys. Rev. B **75**, 155316 (2007).

[34] D. A. Bagrets and Y. V. Nazarov, Phys. Rev. B **67**, 085316 (2003).

[35] C. Flindt, T. Novotny, and A.-P. Jauho, Europhys. Lett. **69**, 475 (2005).

[36] G. Kießlich, P. Samuelsson, A. Wacker, and E. Schöll, Phys. Rev. B **73**, 033312 (2006).

[37] D. A. Bagrets, Y. Utsumi, D. S. Golubev, and G. Schön, Fortschr. Phys. **54**, 917 (2006).

[38] L. Mandel and E. Wolf, *Optical Coherence and Quantum Optics* (Cambridge University Press, 1995), p. 16–20.

[39] S. Gustavsson, R. Leturcq, B. Simovič, R. Schleser, T. Ihn, P. Studerus, K. Ensslin, D. C. Driscoll, and A. C. Gossard, Phys. Rev. Lett. **96**, 076605 (2006).

[40] M. O. Scully and M. S. Zubairy, *Quantum Optics* (Cambridge University Press, 1997), p. 120–137.

[41] C. Emary, C. Pöltl, A. Carmele, J. Kabuss, A. Knorr, and T. Brandes, Phys. Rev. B **85**, 165417 (2012).